Master Thesis
TVVR 15/5013

Sediment transport in Säveån and its implications for erosion and bank stability

Gasper Laurent Sechu

Division of Water Resources Engineering
Department of Building and Environmental Technology
Lund University

Sediment transport in Säveån and its implications for erosion and bank stability

By:
Gasper Laurent Sechu

Master Thesis

Division of Water Resources Engineering
Department of Building & Environmental Technology
Lund University
Box 118
221 00 Lund, Sweden

Water Resources Engineering
TVVR-15/5013
ISSN 1101-9824

Lund 2015
www.tvrl.lth.se

Master Thesis
Division of Water Resources Engineering
Department of Building & Environmental Technology
Lund University

English title:	Sediment transport in Säveån and its implications for erosion and bank stability
Author:	Gasper Laurent Sechu
Supervisors:	Prof. Magnus Larson Dr. Gunnel Göransson
Examiner:	Dr. Rolf Larsson
Language	English
Year:	2015
Keywords:	HEC-RAS, sediment transport, erosion, bank stability, climate change

Acknowledgements

I'm taking this opportunity to express my heartfelt appreciation to my supervisor Professor Magnus Larson, of the Department of Water Resources Engineering, Lund University, for his valuable supervision, guidance and encouragement throughout the whole study.

Special appreciation is extended to my co-supervisor Dr. Gunnel Göransson of the Swedish Geotechnical Institute (SGI), for her valuable assistance in guiding me through the project and providing valuable information.

My sincere gratitude to SGI, Gothenburg office for their facilitation in providing office space, data and a great team of professionals who assisted me at every chance they got.

Lastly I'm profoundly grateful to my family and friends for their financial and moral support throughout the time of my study, without them, I would not have made it this far.

Abstract

This master thesis study is a preliminary investigation of the Säveån River as part of the Swedish Geotechnical Institute's (SGI) landslide risk assessment project. The main objectives include building a hydrodynamic model for the river, estimating sediment transport along the river, assessing the implications for erosion and bank stability and evaluating climate change effects on sediment transport. The study section is from downstream Jonsered hydropower plant to the outlet at Göta Älv. The model selected for the hydrodynamic study is the one dimensional river analysis model HEC-RAS. ArcGIS was used in combination with Hec-GeoRAS to map out the river and extract cross sections from a Digital Elevation Model (DEM) of the river. Steady flow and sediment transport simulations were then done to obtain the hydrodynamics and sediment transport of the river respectively. Model results revealed schematized cross section 12500 close to the upstream end of the study reach to have the most erosion. This section was then used as an example to find the loss in slope stability due to sediment transport using the model SLOPE/W. Climate change simulations were then done with flow data from a simulated period of 2021-2050 and 2069-2098 and compared to a reference period of 1963-1992. Results show that sediment transport is to increase more than twice moving from the reference period to the period 2021-2050 and increase again more than twice from this period to the period 2069-2098 which signifies the end of the century.

Keywords:

HEC-RAS, sediment transport, erosion, bank stability, climate change

Table of contents

Table of Figures

1 Introduction

Sediment transport in rivers and streams has been extensively studied since the 1950's, resulting in various models that are being used to date for load prediction. The major sources of sediment in natural rivers and streams are through overland flow, stream-channel erosion, bank cutting and small erosion channels made in unconsolidated soil (Engelund & Hansen, 1967). Estimates of transport rates in gravel-bed rivers fall between ones that have been developed using formulae and ones that are from sampling campaigns, making the former considerably uncertain and the latter more accurate (Wilcock, 2001). Along with this, there are also difficulties with field measurements which are typically limited in space and time. Some problems of significance associated with sediment transport in rivers and streams include erosion, deposition and reduction in bank stability. Säveån shows signs of bank erosion in some sections which may be attributed to this. In order to solve problems of bank stability, quantification of sediment transported within the river reach is essential and modelling is typically needed due to lack of data.

Erosion and accumulation of sediment in rivers and streams poses risks of bank stability due to varying hydraulic and hydrological flow conditions. Cohesive riverbanks are the most unstable and their instability due to river flow is commonly caused by two processes (Osman & Thorne, 1988). First, due to lateral erosion that increases channel bed width resulting in bank steepening which consecutively reduces stability and second, due to bed lowering that increases bank height also decreasing the stability. The severity of each of the processes is a function of bank material properties, bank geometry, type of bed material, and flow characteristics (Osman & Thorne, 1988). Sections of the river prone to instability require geotechnical solutions to reduce the risk of collapse due to erosion. Sediment transport prediction models aid engineers and planners in determining erosive bank zones to provide erosion protection measures.

1.1 Background

During the period 2009-2011, the Swedish Geotechnical Institute (SGI) has carried out a comprehensive landslide risk investigation thereby creating an inventory in the Göta Älv River valley (SGI, 2012). It was discovered that the

risk for erosion and landslides is already excessive and that it increases with climate change. They have since made brief investigations and inventory of landslide problems along all of Sweden's larger rivers. The purpose of this is to identify and prioritize the 10 most urgent rivers in need of landslide risk mapping, of which Säveån is one. A preliminary assumption is that, the risk of landslides is expected to increase with climate change. In 2013, they began a pilot study in Norsälven to adapt and streamline the methodology utilized in the mapping of the Göta Älv River valley. Additionally SGI prepares mapping of Angermanalven, Säveån and Norrström outlet at Lake Malaren. Along these watercourses societal need for landslide risk assessment is currently of great need. Säveån is now under investigation to provide a basis for erosion and landslide risk mapping.

One of several objectives with SGI is to carry out landslide risk assessment on ten watercourses in Sweden. The goal is to make it safe to live and travel in the country, and provide support to municipalities and county administrative boards with climate change adaptation for safer communities and sustainable development. The outcome with the work is to obtain general landslide risk maps that can be used as a basis for decisions on further more detailed investigations. By delineating the risks, it increases the security of housing and construction within the vicinity of the watercourses.

Under developed climate models, precipitation will increase in Northern Europe, and sea water levels will rise (SGI, 2012). It is required to adapt existing buildings and infrastructure to cope with these changes. Moreover, society needs to take into account the forthcoming climate change and its implications when planning new buildings and infrastructure.

1.2 Objectives

The purpose of the study is to quantify the sediment transport in Säveån, and its implications for erosion and slope stability along the river banks. Spatial and temporal variation in the river and sediment transport is studied from Jonsered Hydropower Station to the outlet at Göta Älv. Limited measurements of the hydrodynamics are available, implying that the river flow must be described through a numerical model. Possible effects of climate change on the flow and sediment transport will also be investigated.

The specific objectives of the project are as follows:

1. Building a hydrodynamic model for the river
2. Estimating sediment transport along the river
3. Assessing the implications for erosion and bank stability
4. Evaluating climate change effects on sediment transport

1.3 Procedure

Prior to addressing the objectives, a review of appropriate literature on sediment transport in rivers with focus on erosive conditions and bank stability was performed. Simultaneously, literature on Säveån, focusing on the hydrological, geological, sedimentological, and morphological conditions was gathered and evaluated in order to gain an understanding of the river and its general behavior. Detailed studies on the river flow and the hydrodynamic characteristics are of special interest.

Available data from Säveån was compiled and analyzed for improved understanding of the river system and in support of subsequent numerical modeling. Data of particular value include the river bathymetry (*e.g.*, cross sections at various locations along the river), time series flow data, water levels, geology and sediment characteristics.

The model HEC-RAS was seen as suitable for carrying out this study. Data extraction was made through HEC-GeoRAS, which is a combination of tools designed to extract spatial data from ArcGIS (Ackerman, 2012). The model was developed to simulate one-dimensional steady flow, unsteady flow, and sediment transport/mobile bed computations in rivers (Brunner, 2010). Although the model is one-dimensional, it can describe complex river cross sections and their variation along the river. The sediment transport capability of the model was tested to simulate the sediment transport and its effect on the river bed and banks based on the hydrodynamics computed by HEC-RAS.

The bank stability due to erosion in time observed due to sediment transport simulations done in HEC-RAS were calculated using the geotechnical software SLOPE/W and eventually flow variation due to climate change scenarios were studied.

Finally, the climate change effects to the sediment transport were studied by simulating climate change data in HEC-RAS and comparing that to climate data from a reference climate period.

1.4 Report content

The main content of the report starts from Chapter 2 and introduces the Säveån, giving its geography, climate, catchment area, flow characteristics, geology and geomorphology, sediment transport, bank erosion and slope failure along the river. Chapter 3 gives the theory behind river sediment transport including basic processes, mechanisms of sediment transport, morphological evolution, bed and bank erosion and slope failure. Furthermore, Chapter 4 gives an overview of the model HEC-RAS, its hydrodynamic capabilities in simulating water levels, flow and sediment transport and morphological change. Chapter 5 highlights the data used for the study which is the flow, water levels and sediment data. Model simulations are given in Chapter 6 and includes topics on the sensitivity analysis, flows and water levels during extreme events, annual sediment transport along the river, river stretches sensitive to long-term erosion, implications of erosion for bank stability and slope failure and climate change effects. And finally, Chapter 7 and 8 wrap up with the discussion and conclusion respectively.

2 Säveån River

2.1 Geography

The Säveån is located in the south west of Sweden within the Västra Götaland County, and flows upstream from north of Borås all the way downstream to the old city of Gothenburg. The river discharges to the Göta Älv and finally discharging into the Kattegat Sea. Figure 2.1 shows the position of the river within Sweden, and zooms in to the catchment.

Figure 2.1: The figure on top shows Sweden (Sverige) from the map of the Nordic countries and on the bottom shows the study area zoomed in to show the delineated Säveån river catchment © Lantmäteriet, Dnr: I2014/00579

2.2 Climatology

The climate in the Västra Götaland County is marked by the maritime influence due to the proximity of the Atlantic and influence of the westerly winds. This means relatively cool summers and mild winters with relatively

high humidity. The sea and its ability to store heat evens out the temperature variations between the seasons and between day and night.
Figure 2.2 and Figure 2.3 show the monthly average temperatures and precipitation respectively for the period 1961 to 1990 to illustrate the climate of the study area.

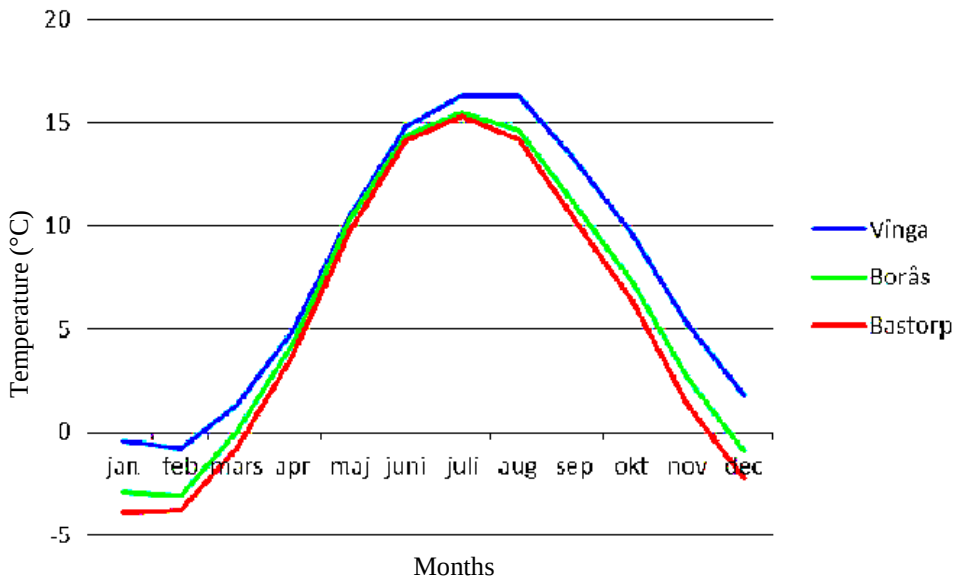

Figure 2.2: Average Monthly Temperatures (°C) for the period 1961-1990 for stations Vinga, Borås and Bastorp in the Västra Götaland County (Persson, et al., 2011)

In the coastal area the average annual temperature maximum, represented here by Vinga is 7.7°C. In Boras, as this may represent the interior, the mean annual temperature is 6.1°C, while Bastorp in the northwestern part of the county the annual mean temperature 5.3°C. During the summer, the temperature difference is relatively small but the winter includes sea-leveling influence. The average temperature for December is 4 degrees lower in Bastorp compared to Vinga (Persson, et al., 2011).

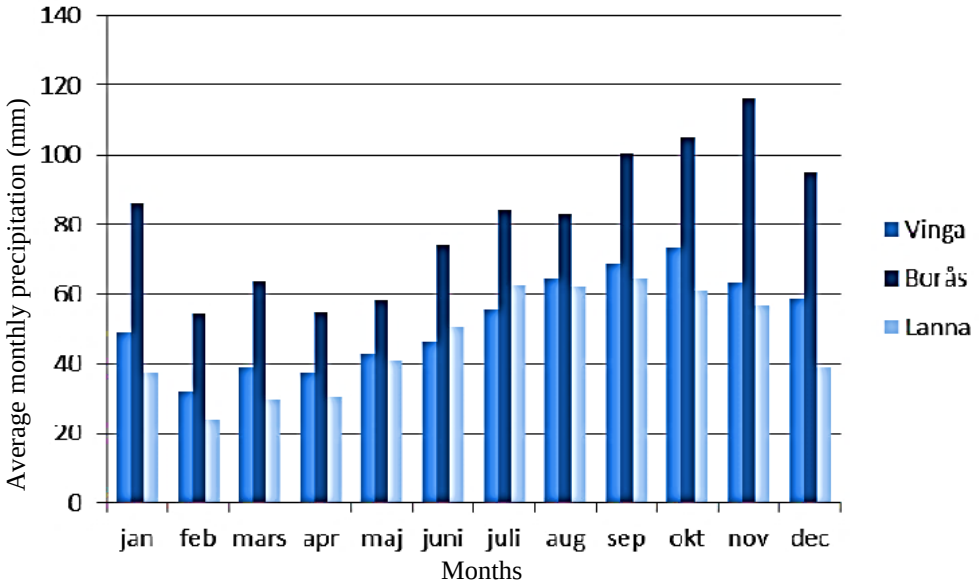

Figure 2.3: Average Monthly Precipitation (mm) for the period 1961-1990 for the stations Vinga, Borås and Lanna in the Västra Götaland County (Persson, et al., 2011)

The estimated annual precipitation is about 800 mm along the coast but increases inland to about 1000 mm and decreases again to around 700 mm around Lake Vänern (Persson, et al., 2011). Figure 2.3 gives the yearly average precipitation for Vinga as 631 mm, 976 mm for Borås and 559 mm for Lanna.

2.3 Catchment area

Säveån is the largest tributary that feeds into Göta Älv. The source for the river is Lake Anten and Lake Säven in the north of Borås. The catchment area measures approximately 1475 km^2 and extends over ten municipalities (Göta älvs vattenvårdförbund, 2006). In comparison to other catchment areas like Lärjeån and Mölndalsån that feed into Göta Älv, Säveån is approximately thirteen and five times bigger respectively and discharges correspondingly higher flows. The river passes through Lakes Mjörn, Sävelången and Aspen and finally flows into the city of Gothenburg, discharging into Göta Älv.

The catchment represents an important natural and recreational area with an ecosystem that is protected (Göta älvs vattenvårdförbund, 2006).

Figure 2.4 shows the Säveån catchment area. Starting upstream at Lake Anten and Säven respectively, the river combines at Lake Mjörn and flows down to Lake Sävelången. It then flows to Lake Aspen and finally down to Göta Älv which discharges to Kattegat Sea.

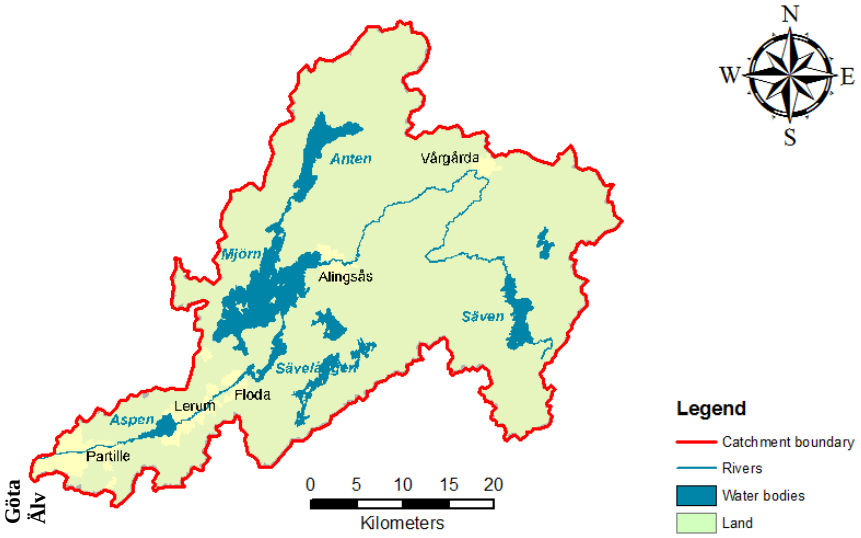

Figure 2.4: Säveån River catchment showing the river network and associated lakes (Länsstyrelserna Västra Götalands Län, n.d.)

The predominant land use is woodland and arable lands occupying 57% and 10.8% of the area respectively. Other land uses include logging (1.9%), peat land (3%), lakes (10.1%), pastures (4%), buildings (5.1%) and others (8.1%). The river is also known for extensive recreational fishing with mostly salmon (Göta älvs vattenvårdförbund, 2006).

The modelled stretch i.e. from downstream Jonsered hydropower station to the outlet at Göta Älv was selected due to availability of continuous river bathymetry data. The data was available for the whole section, in contrary to further upstream which had sections that this data could not be collected due to ecological reasons. This was then taken as the suitable stretch for testing the model and performing method development.

2.4 Flow characteristics

The average flow for the whole river is about 18 m^3/s but the data gave flows to a maximum of 108 m^3/s and minimum of 1 m^3/s. However, the average flow of 24 m^3/s is used for the study since it is the flow that covers the study area that extends only from Jonsered to the outlet at Göta Älv. The reason behind this value is that it is an average of the flow data from 2006 to 2010 used in this study. This stretch was selected mainly due to consistency in bathymetric data that covers the whole stretch as opposed to further upstream that has missing data. Between Floda and Lerum, is a head difference of about 40 meters favoring hydropower production in some places (Göta älvs vattenvårdförbund, 2006). Notable hydropower plants starting upstream include Solveden with 1240 kW, Floda with 360 kW, Hillefors with 160 kW, Hedefors with 2800 kW and Jonsered with 2357 kW of installed power (Jersby, 2007), as seen in Figure 2.5.

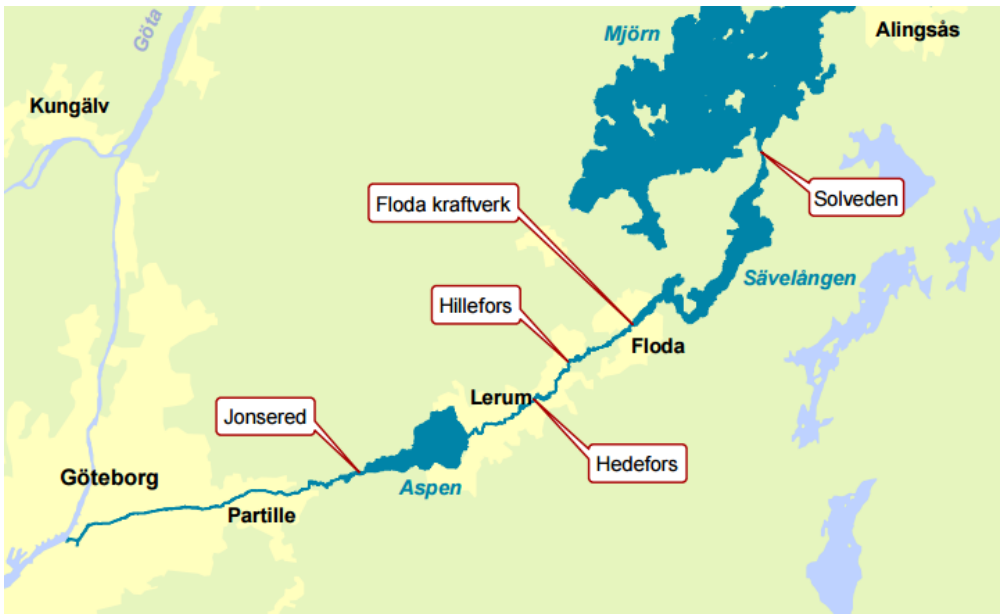

Figure 2.5: Hydropower plants along Säveån River, starting upstream with Solveden to downstream with Jonsered (Länsstyrelserna Västra Götalands Län, n.d.)

2.5 Geology and geomorphology

The principal soil is dominated by clayey sediments (cohesive sediments) with elements of sand, silt and glacial fluvial deposits. Most of the surficial sediments are post glacial, settled in a marine environment and many interesting landscapes have been created along the river as canyons are formed when it cuts down the clay sediments (Göta älvs vattenvårdsförbund, 1973-2004). Geological and geomorphological surveys along the Säveån watercourse were carried out by the Swedish Geological Survey (Sveriges geologiska undersökning, SGU) as part of the landslide risk mapping by SGI. The surveys were carried out between Gothenburg and Nääs Castle just upstream of Lake Sävelång (Engdahl & Påse, 2014).

The bedrock morphology entails of a rift valley that is particularly affected by developments during the Mesozoic geological era 245 – 65 million years ago (Lidmar-Bergström, 1998). The mountain is chipped rift and follows a clear pattern as seen in Figure 2.6. Central to the figure is the Göta fault oriented north-south and can be traced from Vänern to Kungsbacka. There are also canyons that are oriented roughly east-west and forms Säveån valley and parts of Lärjeåns and Mölndalsåns valleys (Engdahl & Påse, 2014).

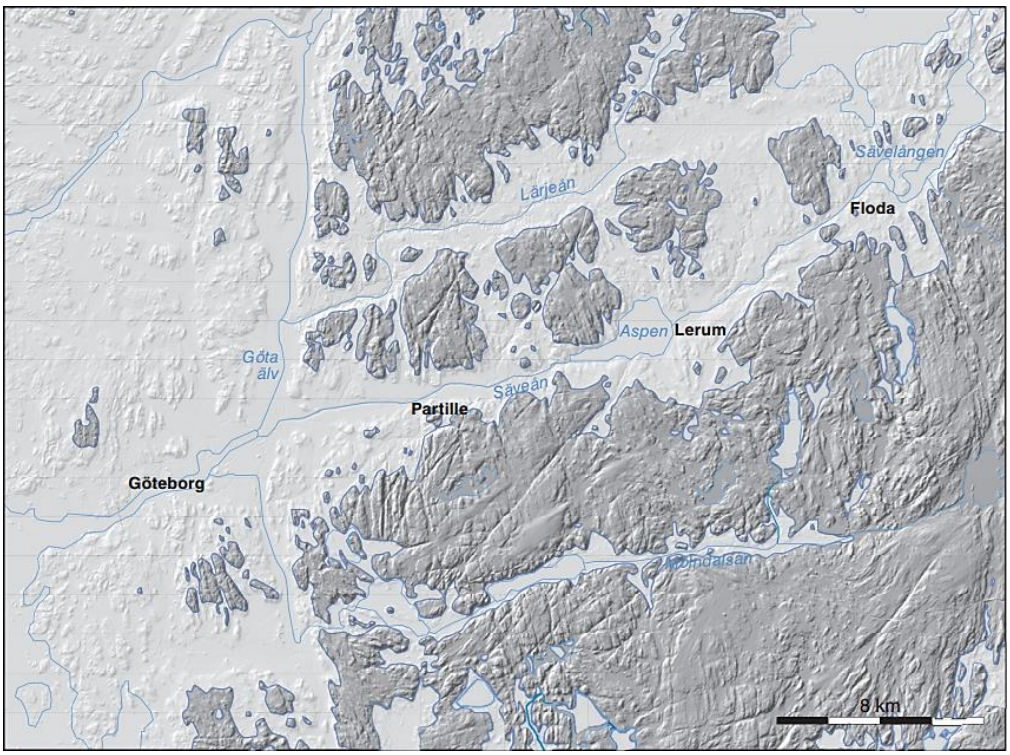

Figure 2.6: Areas below and above the highest coastline and lakes lying over the highest coastline. The map shows the distribution of sea and country about 13,500 years ago (Engdahl & Påse, 2014)

The westernmost parts of Säveån valley became ice-free around 14,500 years ago. Lerum was ice free about 14,000 years ago and the western part of the lake Sävelången became ice-free about 13 700 years ago (Engdahl & Påse, 2014).

There are sediment plans of different ages occurring along the Säveån. The oldest and highest surfaces exhibit traces of severe erosion while the younger lower located surfaces are almost completely intact and in some cases are marked by very young sediments. This makes it easier to divide the valley into different areas to understand the layout better. SGU therefore divided the valley section between Gothenburg and Lake Sävelången into six different environmental zones based on soils, soil depth and erosion conditions as given in Figure 2.7 (Engdahl & Påse, 2014).

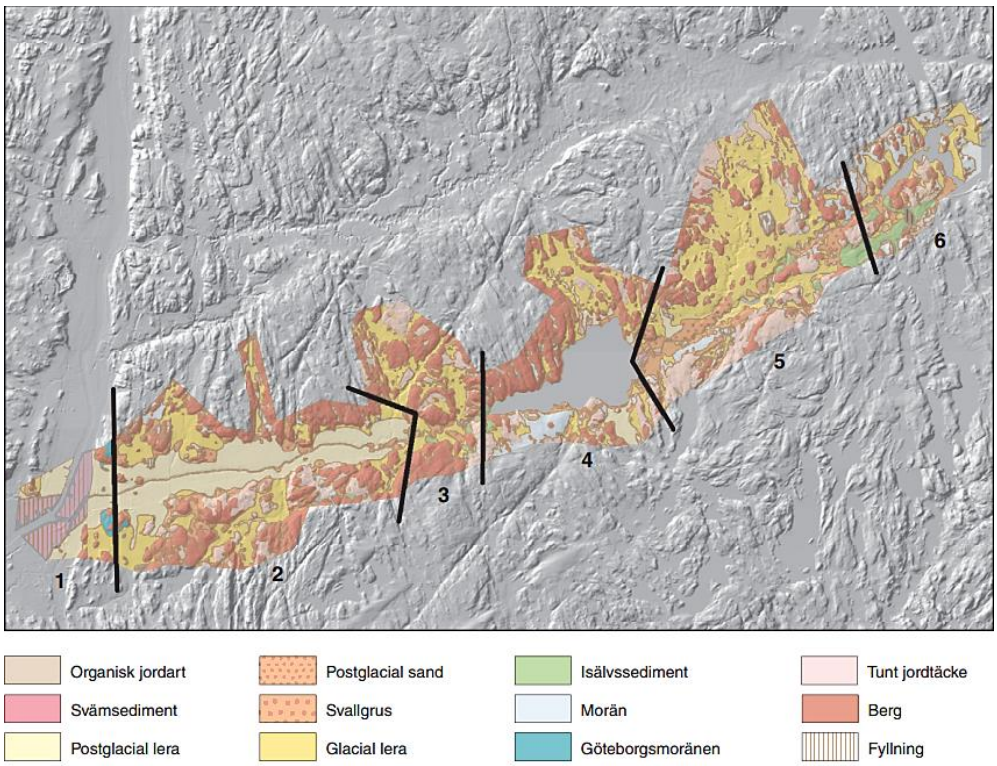

Figure 2.7: Subdivision of the Geological environmental zones along Säveån western part (Engdahl & Påse, 2014)

From the figure, area 1 is located downstream where the Säveån discharges to Göta Älv, and consists of a clay layer of up to about 90 m of which 10 m is post-glacial clay. Also, a large part of the area is populated with industries, storage buildings and multi-family residents resulting in the clay being covered with aggregate. Area 2 stretches between Gamlestaden and just west of Kåhog and forms fine-grained soils (mostly post-glacial) with a flat plane between 3 to 10 m above sea level. Area 3 covers the stretch between Kåhog and Jonsered and consists of post-glacial sand and glacial clay in the soil surface. The topography is hilly and there are some steep slopes down against Säveån in which landslide and ongoing erosion occurs. Area 4 covers the outcrops of the north of Lake Aspen and the moraine south of the lake. In the side valley to the north is glacial clay that has traces of ravines and small landslides. The thickness of the clay is believed to be 10-20 m in this area. Southeast of Lake Aspen is post-glacial clay with no traces of landslides and ravines. Area 5 is between Lerum's northeastern part and Floda and here

Säveån has eroded from the post-glacial sand to the underlying glacial clay. The thickness of the soils is greatest closest to Lerum center reaching about 30-50 m. Traces of ravines and landslides are visible, as well as ongoing erosion in slopes down towards the river. In area 6 along Lake Sävelång beaches are glacial clay with an estimated thickness of 5-10 m. Clay soils are leaning slightly towards the lake, and only a few canyons and landslides occurs in this area (Engdahl & Påse, 2014). This study only covers the river stretch within area 1, 2 and 3.

2.6 Sediment transport, bank erosion and slope failure

Sediment transport and erosion is still not taken as a severe environmental degradation in Sweden, except on a local scale for example agricultural lands and vegetation removal as a result of construction activities. The reason for this is the small amounts of erosion that are caused by small intensities of rainfall and snowmelt (Brandt, 1990).

As stated earlier, the major sources of sediment in natural rivers and streams are through overland flow, stream-channel erosion, bank cutting and small erosion channels made in unconsolidated soil (Engelund & Hansen, 1967). The focus of this study is on the sediment derived from channel erosion, i.e. sediment coming from bed and banks of the river and therefore contribution from overland flow is not included.

In the Säveån, no measured data for the sediment transport exists, but the river shows clear signs of erosion as seen in Figure 2.8 which shows one of the eroded zones within the study area. Channel erosion within the study area is most visible at area 3 of Figure 2.7. The eroding banks are clear signs of erosion due to sediment transport. The link between the erosion due to sediment transport and slope stability will be the focus of this study.

Figure 2.8: Säveån River within the study section showing erosion of the banks (Photo by Gasper Sechu)

3 River Sediment Transport

3.1 Basic processes

Sediment transport in rivers comes in one of three forms namely bedload, suspended-load or wash load transport. The bedload transport is essentially movement of sediment particles (rolling or sliding) along the bottom of the river. With bedload transport, the shear stress is of importance due to sediment contact with the bottom of the river surface. Suspended load is the part of sediment particles that is suspended within the water column. This is part of the load that was once bedload but due to increased shear stress and initiation of motion, the sediment particles are lifted and suspended in the water column. The particles are sustained by turbulence which in turn develops sediment concentration profiles. Finally, the wash load is the portion of sediment that is carried by the river flow such that it remains in suspension or close to the water surface. Figure 3.1 below gives an illustration of sediment bedload and suspended load due to incipient motion.

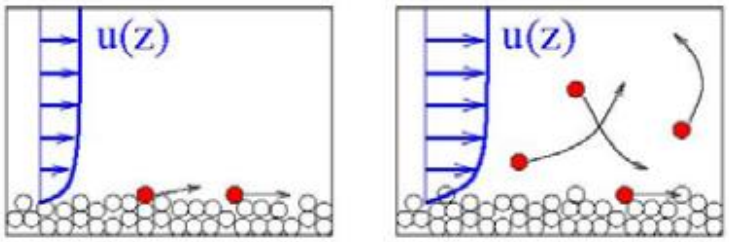

Figure 3.1: To the left is the sediment bedload and the right is the suspended load due to initiation of motion (Camenen & Larson, 2007)

3.2 Mechanics of sediment transport

In sediment transport studies, it is always crucial to first reflect on the flow condition in which particles start to move, this is known as incipient motion. The incipient motion can be obtained from a balance of forces or moments derived from the forces (Figure 3.2) acting on a sediment particle at the bottom of the river (Yang, 1977). It is always important to separate the shear stress generated by the flowing water and the shear stress required to move the sediment grain, when the former exceeds the later transport occurs. At incipient motion, the sediment particle exhibits bedload transport, it is with

additional stress and turbulence that the particle is lifted to exhibit suspended load transport.

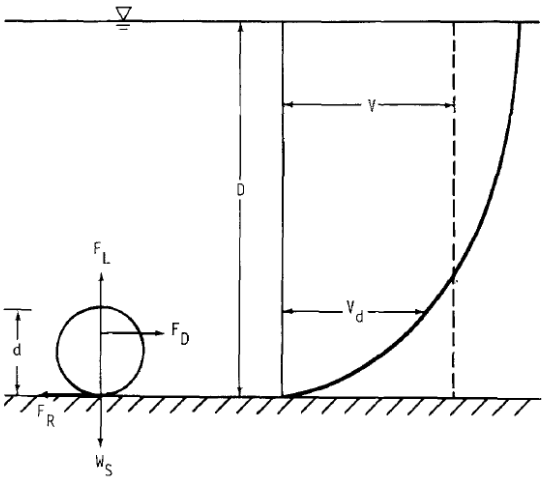

Figure 3.2: Sediment particle at the bottom of the river bed with forces acting (Yang, 1977)

The forces or moments can be obtained by the shear stress or the velocity approach. By the shear stress approach, the shear stress occurring at the bed of the open channel is the tug of water on the wetted perimeter. For a uniform flow, this can be expressed as follows:

$$\tau = \gamma RS \qquad (3.1)$$

Where:

τ = average shear stress (Pa)
γ = specific unit weight of water (N/m^3)
R = hydraulic radius (m)
S = surface slope of water

The most widely used analyses for incipient motion are derived from the shear stress approach; these are Shields (1936) and White (1940). Shield's diagram approach (Figure 3.3) is used in HEC-RAS for particle incipient motion.

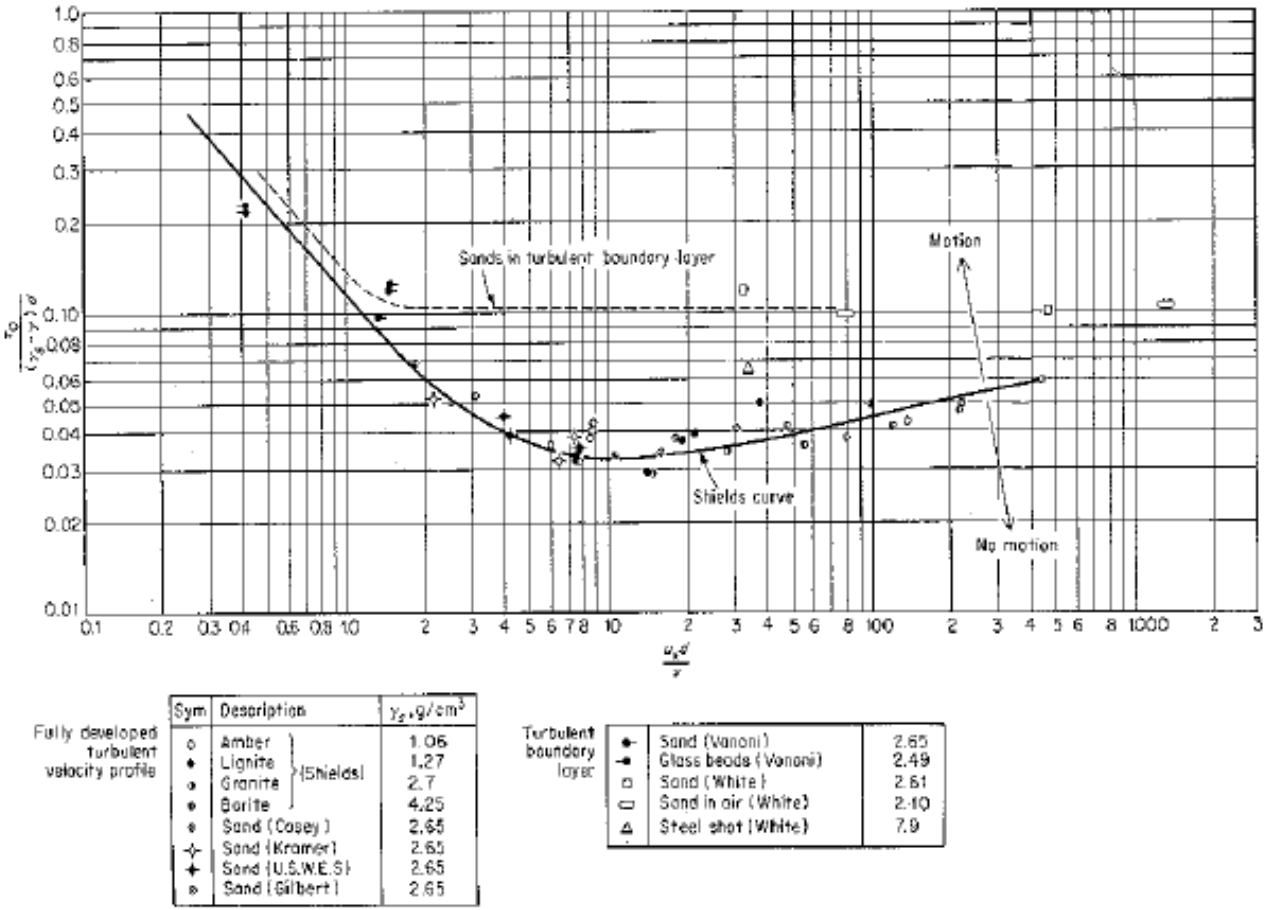

Figure 3.3: Shield's Diagram, Graf (1971) applied for incipient motion in HEC-RAS (Brunner, 2010)

The velocity approach on the other hand has been tried out experimentally and works on the principle that the drag acting force on a particle is comparative to the square of the relative velocity between the fluid and particle. Neil (1967), Bogardi (1968) and Yang (1973), amongst others have developed various equations for the incipient motion based on the velocity approach.

3.3 Morphological evolution

Morphological evolution of rivers and streams is the change of the shapes of rivers and streams with time. This is mainly caused by the gradients in the sediment transport rate that yield erosion and deposition within a river reach. Exner (1920) and (1925) was the first to formulate quantitatively the morphodynamic problem in quantitative terms. Figure 3.4 illustrates mass conservation of a unit width of a river bed with x denoting the flow direction. From the figure, η is the bed elevation, q_b is the volume transport rate of bedload sediment per unit width per unit time, D_s is the deposition rate and E_s is the erosion rate (Chaudhry, 2008).

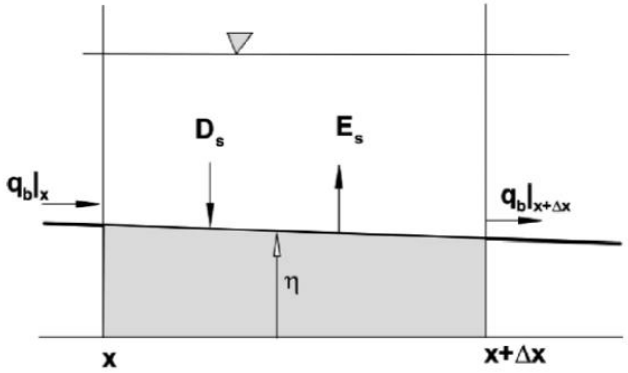

Figure 3.4: Mass conservation at the river bed (Chaudhry, 2008)

This can be expressed mathematically through an equation known as the Exner equation and is given as:

$$\left(1-\lambda_p\right)\frac{\partial \eta}{\partial t} = -\frac{\partial q_b}{\partial x} + D_s - E_s \qquad (3.2)$$

Where: λ_p = the bed porosity in the control volume

The Exner equation can be used to describe erosion and deposition using the gradient in the sediment volume transport rate such that

- For erosion to occur:

$$\frac{\partial q_b}{\partial x} > 0 \tag{3.3}$$

- And for deposition to occur:

$$\frac{\partial q_b}{\partial x} < 0 \tag{3.4}$$

3.4 Bed and bank erosion

Erosion is a natural and important part in a natural system. However, it becomes a problem in areas that people have settled leading to anthropogenic activities that disturb the pristine environmental system. The erosion of a river or stream bed (also known as scour) and banks can also be associated with sediment transport. Different river geometry features play a part in the erosion and deposition of sediment. Velocity gradient plays a part in the erosion of the bed and banks such that:

$$\frac{dV}{dx} \geq 0 \rightarrow \frac{dq_b}{dx} > 0 \rightarrow Erosion \tag{3.5}$$

Where: V = flow velocity

This can be described as, when the velocity gradient is greater or equal to zero, it then implies that gradient of the volume transport rate is greater than zero, which has the effect of erosion along that stretch.

In addition to this, in river meander bends transversal currents occur such as spiral currents which affect the velocity gradients, the transport rate and therefore the erosion. Meander bends are the sections of the river that the prevailing direction of velocity is not necessarily in the x-coordinate. But since HEC-RAS is a one dimensional flow model, it assumes the primary component of velocity in the x-coordinate (Kasper, et al., 2005).

Bank erosion is most evident in river bends during the formation of meanders. When flow goes around a bend, sediment is eroded on the outer part at the same time deposited on the inner part. Continual ongoing of this coupling process forms meanders that become more and more pronounced until at one point the river short circuits by finding a shorter path through bypassing the meander and a new formation known as an oxbow lake is formed as seen in Figure 3.5.

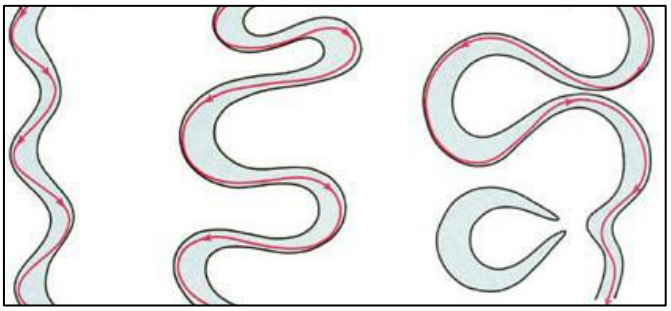

Figure 3.5: Formation of meanders (center) and an oxbow lake (right) due to erosion and deposition in a river bend (Schieber, n.d.)

3.5 Slope failure

To determine the risk of slope failure, we must study slope stability, which is sometimes expressed as the forces acting on the slope. The forces in play are driving forces which act to move the earth material down the slope and resisting forces which oppose the movement. The most common driving force is the downslope component of the weight of the slope material, including anything superimposed on the slope e.g. structures, vegetation or fill material. The most common resisting force is the strength, or resistance to failure by sliding or flowing, of the slope material acting along potential slip planes (Keller, 2011).

Common failure in slopes includes plane, wedge, toppling, rockfall and rotational (circular or non-circular) (Figure 3.6). Plane, wedge, toppling and rockfall are common in rock formations and the main controlling factor is the orientation and spacing of discontinuities in the planes with respect to the slope face. Rotational failures (circular or non-circular) are common in

materials such as soils, mine dumps, heavily jointed or fractured rock mass and very weak rocks. The key controlling factor for these failures is the material properties, water content and foundation strength (Rai & Singh, n.d.). Since the soil in the Säveån is mostly clay, rotational slope failure is used.

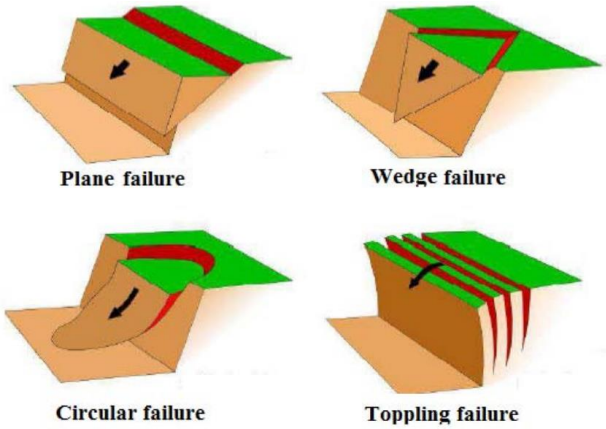

Figure 3.6: Common types of slope failures ((Rai & Singh, n.d.)

4 HEC-RAS model

4.1 Model overview

The Hydrologic Engineering Center's River Analysis System (HEC-RAS) is a one dimensional river analysis model that can make calculations for steady, unsteady flow, sediment transport or water temperature modelling (Brunner, 2010). The model can perform calculations for both prismatic and natural channels. It is free software that has been developed by the US Army Corps of Engineers to aid water engineers and planners.

The river analysis components within HEC/RAS include steady flow water surface profile computations, unsteady flow simulations, sediment transport simulations and water quality analyses. A common factor for all the four simulation routines is that all adopt the same geometric representation of the river system. Additionally, the model contains some hydraulic design features that can be used once the water surface profiles are computed (Brunner, 2010). For the current study, the model was utilized to perform steady flow simulations and sediment transport computations. The two features are explained in the following subsections.

4.2 Water level and flow

4.2.1 Steady flow water surface profiles

The water surface profile is calculated from one cross section to the other through the Energy equation using an iterative procedure known as the standard step method. The energy equation taken at point 1 and 2 is given as follows:

$$Z_2 + Y_2 + \frac{a_2 {V_2}^2}{2g} = Z_1 + Y_1 + \frac{a_1 {V_1}^2}{2g} + h_e \qquad (4.1)$$

Where: Z_1, Z_2 = elevations of the main channel inverts
$Y_1 Y_2$ = water depth at cross section 1 and 2 respectively
$V_1 V_2$ = average flow velocities
$a_1 a_2$ = velocity weighting coefficients
g = acceleration due to gravity

h_e = energy head loss

The terms of the energy equation are depicted in Figure 4.1.

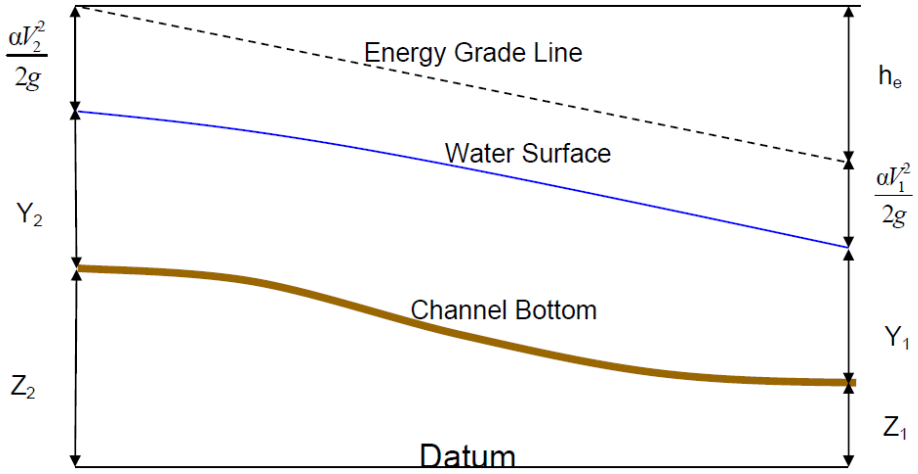

Figure 4.1: Depiction of the energy terms (Brunner, 2010)

Energy losses consist of frictional losses as well as contraction or expansion losses. The energy head loss is given as follows:

$$h_e = L\bar{S}_f + C\left|\frac{a_2 {V_2}^2}{2g} - \frac{a_1 {V_1}^2}{2g}\right| \qquad (4.2)$$

Where: L = discharge weighted reach length
$\bar{S}_f$ = Characteristic friction slope between cross sections
C = Expansion or contraction loss coefficient

The distance weighted reach length, L is computed as:

$$L = \frac{L_{lob}\bar{Q}_{lob} + L_{ch}\bar{Q}_{ch} + L_{rob}\bar{Q}_{rob}}{\bar{Q}_{lob} + \bar{Q}_{ch} + \bar{Q}_{rob}} \qquad (4.3)$$

Where: L_{lob}, L_{ch}, L_{rob} = reach lengths for cross sectional flow in the left overbank, main channel and right overbank
$\bar{Q}_{lob}, \bar{Q}_{ch}, \bar{Q}_{rob}$ = mean of the flow between sections for the left overbank, main channel and right overbank

The friction slope is calculated as:

$$\bar{S_f} = \left(\frac{Q_1 + Q_2}{K_1 + K_2}\right)^2 \quad (4.4)$$

Where: $Q_{1,}Q_2$ = flows at the two cross sections (which is the same for steady flow)

K_1, K_2 = conveyance at the two cross sections which is given as:

$$K = \frac{1}{n} AR^{2/3} \quad (4.5)$$

Where: n = manning's coefficient of roughness

A = cross sectional flow area

R = Hydraulic radius

Finally, for steady flow, the continuity equation is used as well in solving for the velocity and water surface profile. This states that the flow at any section is constant and is given mathematically as:

$$Q = AV \quad (4.6)$$

Where: Q = river flow

A = sectional area

V = flow velocity

Values for flows are needed for each cross section in order calculate the water surface profiles. These should be specified from upstream to downstream for each reach. For a given river system, at least one value of flow should be entered for each reach. For steady flow, when a flow value is entered, it stays constant until another value is encountered within the same reach (Brunner, 2010).

4.2.2 Boundary condition for steady flow

Boundary conditions are required to form initial water surfaces profiles at the extremes of the river system (upstream and downstream). Three flow regimes are possible in steady flow simulations namely subcritical, supercritical and

mixed. In a subcritical flow profile, boundary conditions are only essential at the downstream end of the river. For a supercritical flow profile, boundary conditions are essential at the upstream end and for a mixed flow profile, they must be entered at both upstream and downstream ends of the river reach (Brunner, 2010). Boundary conditions in a steady flow profile include:

- Known water surface elevations,
- Critical depth,
- Normal depth, and
- Rating curve

4.3 Sediment transport and morphological change

There is a lot of uncertainty to sediment modelling in HEC-RAS due to uncertainty in the data for bed change calculation and the empirical nature of applied functions which are highly sensitive to physical variables (Brunner, 2010). Data required in simulating a mobile bed change in HEC-RAS includes the river geometric data, a quasi-unsteady flow plan which also includes temperature data and sediment data. The geometric data essentially consists of the river topology, cross section bathymetry, river banks and any other hydraulic structures present in the river system. The calculation procedure for sediment transport in HEC-RAS can be schematically described as follows:

4.3.1 Quasi-unsteady flow

HEC-RAS uses hydrodynamic simplifications for mobile bed transport by implying a quasi-unsteady flow assumption rather than an unsteady flow which would take a longer computation time. The quasi-unsteady flow technique applies a series of discrete steady flow profiles which remain constant for given time intervals. In the future it has been planned to release a version of the sediment model that uses unsteady flow procedure to approximate the mobile bed transport. The steady flow profiles are further divided into three time steps for sediment transport calculations, the flow duration, the computation increment, and the mixing time step. (Brunner, 2010).

4.3.2 Calculation time steps

The flow duration time step is the biggest time step and depicts the time length over which stage, flow, temperature or sediment loads are taken as constant. For example if the discharge data was collected at daily intervals, the flow duration will be 24 hours unless the data consists of smaller time steps that were interpolated (Brunner, 2010).

The flow duration is divided further to get the computation increment. This is the time step that the hydrodynamics and bed geometry are updated. It can be sensitive to the model and lead to instability since the bed geometry is only updated at the end of the time step. If it is too long, the bed geometry will not be updated as frequent and can lead to varying results (Brunner, 2010). Figure 4.2 shows the depiction of the two time steps as used in HEC-RAS mobile bed computations.

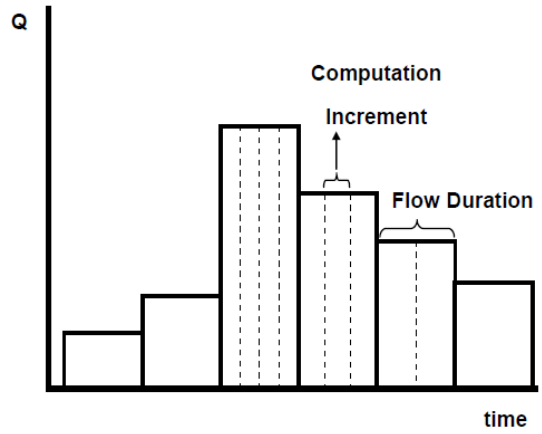

Figure 4.2: The quasi-unsteady flow series showing the flow duration and computation increment time steps (Brunner, 2010)

The computation increment is also divided into the bed mixing time step. In a mixing time step within a computation increment, the hydraulic parameters, bathymetry and transport potential remain the same. Changes that take place are the calculations for the sediment erosion and accumulation (Brunner, 2010).

4.3.3 Sediment continuity

The HEC-RAS sediment model uses the Exner equation as given below:

$$(1-\lambda_p)B\frac{\partial \eta}{\partial t} = -\frac{\partial Q_s}{\partial x} \qquad (4.7)$$

Where: B = channel width
η = channel elevation
λ_p = porosity of the active layer
t = time
x = distance
Q_s = conveyed sediment load

The equation uses the principle of mass conservation in a given control volume for solving the sediment continuity equation, it implies that the change of sediment volume that enters a control volume, equals the difference between incoming and outgoing sediment loads. The control volume is taken at each cross section and the principle works by comparing transport capacity to supply of sediment. If the former is greater than the latter it then results in sediment deficit viewed as eroding beds. Vice versa gives a sediment surplus leading to accumulation.

4.3.4 Transport functions

Various transport functions exists in HEC-RAS and can be chosen according to specific needs. The most common parameter for selection of a transport function is the distribution of the grain size from a sieve analysis. This is because the transport functions have been developed for a range of grain size applications. There are seven different transport functions to choose from, and these are:

- Ackers and White (1973)
- Engelund Hansen (1967)
- Laursen-Copeland (Copeland & Thomas, 1989)
- Meyer-Peter & Müller (1948)
- Toffaleti (1968)
- Yang (1973) and (1984)

- Wilcock (2001)

The transport function adopted for this study is the Meyer-Peter Müller which is based on experimental data and has years of use for rivers with coarse sediments. The principle is that the transport rate is proportional to the difference between the mean shear stress acting on the grain and the critical shear stress. The applicable range of particle sizes is 0.4 to 29 mm and can be used for well-graded sediments (Brunner, 2010). But due to the nature of fine sediments within the river, along with Meyer-Peter Müller, an approach for estimating sediments within the silt and clay sized ranges known as Krone (1962) and Parthenaides (1962) was used.

The equation for Meyer-Peter Müller is given as:

$$q_b^* = 8(\tau^* - \tau_c^*)^{3/2} \quad , \quad \tau_c^* = 0.047 \tag{4.8}$$

Where: q_b^* = dimensionless volume bedload transport rate per unit channel width (Einstein number)
τ^* = dimensionless boundary shear stress (Shields number)
τ_c^* = dimensionless critical shear stress

Krone and Parthenaides experiments combine deposition and erosion respectively using the assumption that cohesive particles are too small that their behavior is primarily influenced by surface forces rather than gravity. Krone deposition's fundamental concept is that a floc will stick to the bed contrary to sand and gravel that sink to the bed. Likewise, Parthenaides erosion observes whether the bed shear stress is adequate to overcome the electrochemical forces holding the grains together instead of using the bed shear stress capability to lift a grain particle off the bed. These two functions are used in HEC-RAS to calculate the deposition and erosion of cohesive sediments (Brunner, 2010). The Krone and Patheniades functions are given below respectively with subscript d and e representing deposition and erosion:

$$\left(\frac{dC}{dt}\right)_d = -\left(1 - \frac{\tau_b}{\tau_c}\right)\frac{V_s}{y} \tag{4.9}$$

Where: C = concentration of sediment

t = time
τ_b = bed shear stress
τ_c = critical shear stress for deposition
V_s = fall velocity
y = water depth

$$\left(\frac{dm}{dt}\right)_e = M\left(\frac{\tau_b}{\tau_c} - 1\right) \quad (4.10)$$

Where: m = mass of material in the water column
M = empirical erosion rate for particle scour
Other variables as in deposition function

The two functions combine together to form part of the general basis that controls transport of cohesive sediments within three hydrodynamic states namely deposition, particle erosion and mass erosion (Figure 4.3). These states are separated by two threshold shear stresses, the critical shear threshold for particle erosion (τ_c) and the critical shear threshold for mass erosion and these are specified by the user in HEC-RAS (τ_m) (Brunner, 2010).

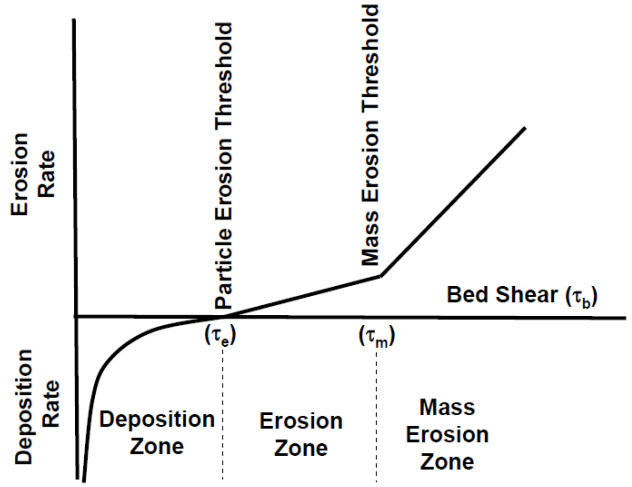

Figure 4.3: Cohesive sedimentation zones as a function of shear stresses (Brunner, 2010)

The threshold values specified for this project were obtained from compilations done by Partheniades (2010) from his previous experiments on

erosion of cohesive soils. These were done with mud from the San Francisco Bay similar to the one's used in Krone's (1962) studies using flume experiments. The results are summarized in Figure 4.4 which gives the two types of beds that were tested i.e. series I and series II. Series I beds are placed beds with natural water content and series II beds are deposited beds created by deposition and consolidation of suspended sediments at low velocities. Series II was more applicable for the use of this project since sediments in river flow are deposited and consolidate naturally when flow reduces.

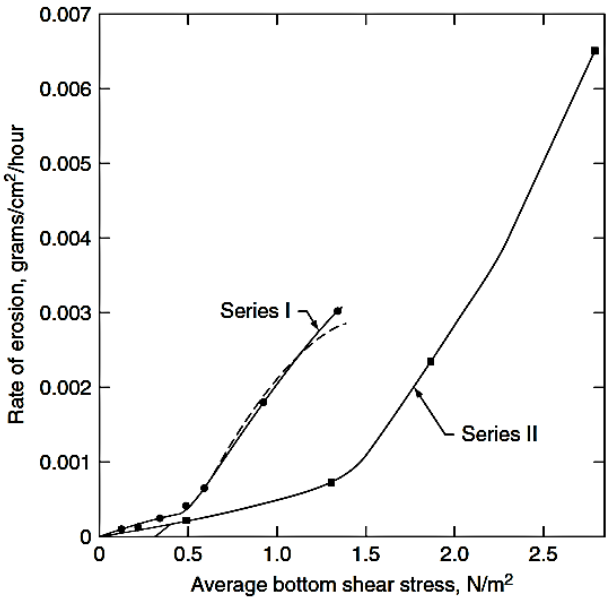

Figure 4.4: Shear stress rate of erosion for dense bed of San Francisco Bay mud (Partheniades, 2010, p. 197)

Using the Partheniades erosion model in Figure 4.4, the values for τ_c and τ_m used in the HEC-RAS model were 0 and 1.5 N/m^2 respectively and therefore corresponding erosion rates of 0 and 0.001 grams/cm^2/hour for the particle erosion and mass erosion thresholds respectively.

4.3.5 Fall velocity

Meyer-Peter Müller transport function does not use fall velocity but it is used in Krone's deposition. Fall velocity theories usually start with an initial assumption of force balance on a particle falling freely in a water column,

taking an upward drag force and a downward gravitational force corrected for buoyancy. There are four options for fall velocity methods in HEC-RAS which are Rubey, Toffaleti, Van Rijn and Report 12.

Rubey avoided the initial assumption, had an initial guessed property and created a simple analytical equation for the fall velocity. Toffaleti on the other hand created empirical curves using the initial force balance dependency. Van Rijn started off with Rubey as an initial assumption and calculated fall velocity using experimental curves that are founded on the Reynold's number. Lastly, Report 12 uses iterative results that are derived from the Van Rijn curves (Brunner, 2010). For this study, the Rubey fall velocity was used since it has been shown to be adequate for silt, sand and gravel grains (Brunner, 2010).

4.3.6 Sorting method

HEC-RAS has included two algorithms to mimic the bed sorting and armoring namely Exner 5 and Active Layer Method, see Figure 4.5. Exner 5 is a three layer mixing method which is the default in HEC-RAS and the Active Layer Method is a simpler two layer mixing method. For this study, Exner 5 was adopted.

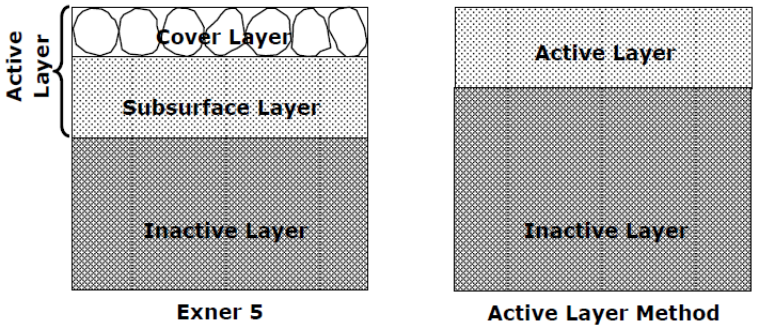

Figure 4.5: Section through the two mixing layers for the sorting and armoring in HEC-RAS (Brunner, 2010)

4.3.7 Boundary conditions for sediment transport

Sediment boundary conditions included with HEC-RAS include rating curve, sediment load series and equilibrium load. Rating curves give the sediment load with the corresponding flow at the point of measurement and can be

used for cross sections with available sediment and flow measurements. Sediment load series on the other hand is a sediment load that is not tied to a flow boundary. Since this boundary is not tied to a flow, measured sediment load can be used in any of the cross sections except the downstream one. And equilibrium load is a condition set that sediment load equals the capacity and due to this there will be no aggradation or degradation at the particular cross section. Due to lack of sediment data for the Säveån and a pre-requisite of an upstream boundary, this was set as an equilibrium load boundary.

5 Data used for the study

5.1 Flow data as upstream boundary

The model HEC-RAS requires upstream or downstream boundary conditions depending on the simulations that are being run. The flow data for the study section is obtained from a gaging station downstream of the hydropower station Jonsered. The data has been logged in by the Swedish energy company Vattenfall at a 12 hour intervals. The range acquired for the study is from 2006-01-10 to 2010-12-31, and varies significantly such that the minimum, mean, median and maximum values are 1, 24, 20 and 108 m^3/s respectively, due to seasonal changes and flooding events as visualized in Figure 5.1. Various flooding events are recorded by the graph, but a particular flooding event occurred around December 2006 that was not properly registered by the gaging station due to over toppling of the measuring gauge, giving flow values less than what actually occurred.

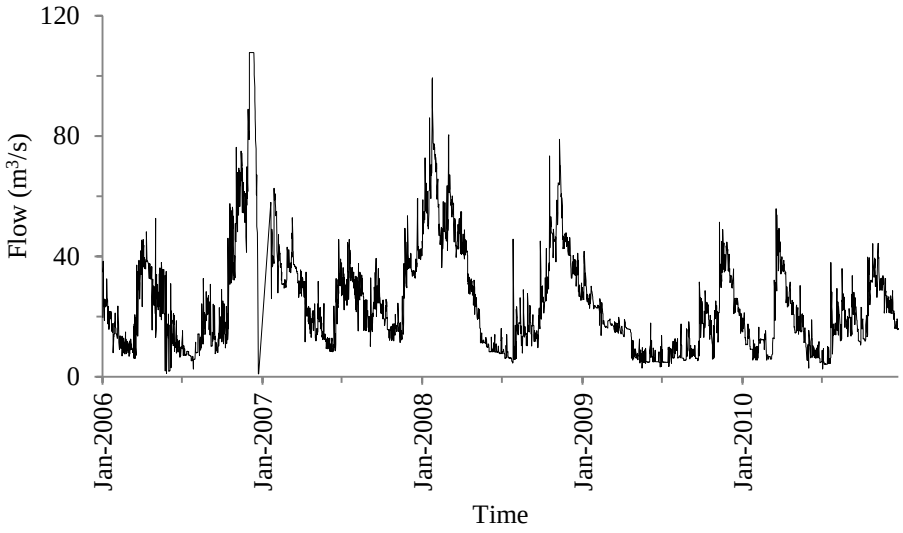

Figure 5.1: Time series river flow data for Säveån taken at a gaging station downstream of Jonsered hydropower station used as the upstream boundary condition for the study section

Table 5.1 gives the total yearly runoff and mean flow volume computed from the Säveån flow data. The data revealed that the year 2008 had the most flow and the year with the least flow was 2009.

Table 5.1: Total yearly runoff volume and mean flow for the Säveån study section

Year	Total Runoff (m^3/year)	Mean Flow (m^3/s)
2006	826,044,524	27
2007	782,026,813	27
2008	1,047,331,531	33
2009	513,939,531	16
2010	585,406,917	19

The gaging station also gives water level and river flow relationships (flow rating curve). Figure 5.2 shows a flow rating curve generated from plotting all water levels versus flow for the whole time series and this is based on measurements done in the early 20th century. However, the building of bridges, erosion protection, etc., may have affected the relationship between the two, which may explain the dots outside the curve.

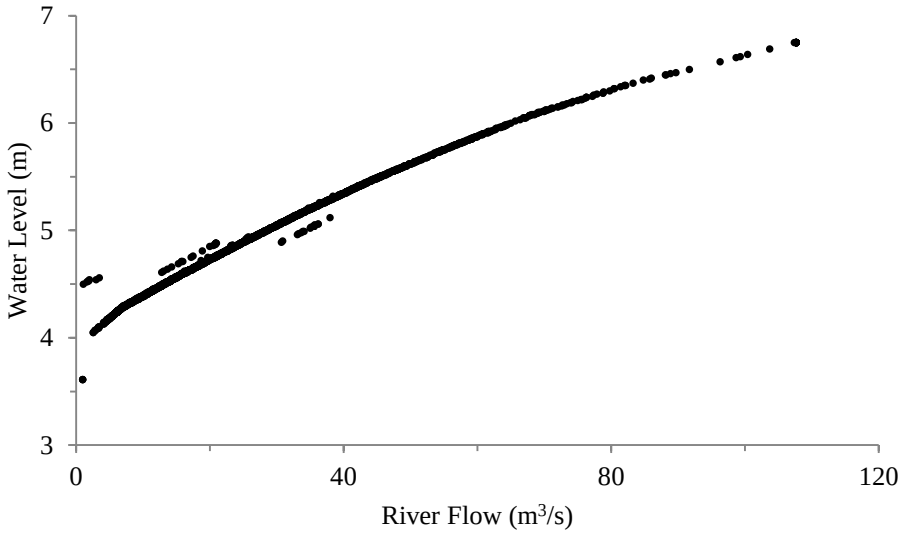

Figure 5.2: Flow rating curve for the gaging station just downstream of Jonsered hydropower station

The flow data is used as input for the upstream boundary of the HEC-RAS model. The flow mean, maximum and entire time series is used in the simulations for different purposes.

5.2 Flood frequency analysis

Flood frequency analysis was done using the upstream flow data from Jonsered, to determine the 50 and 100 year return period floods to be used in the simulation of the hydrodynamics and sediment transport. Since data was available from 2006 to 2010, only five annual peak flows were available for this. The analysis was done using the Gumbel distribution given in Figure 5.3. Gumbel probability distribution has been widely used in the prediction of hydrological maximum events due to its prediction accuracy.

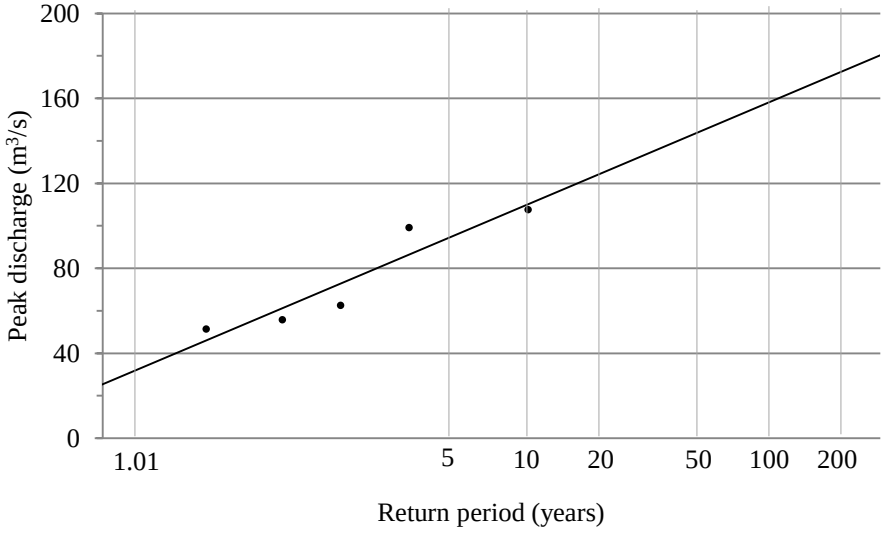

Figure 5.3: Gumbel extreme flood analysis for flows from year 2006 to 2010

The five maximum flow data were extrapolated in the Gumbel paper to get estimates of discharges at the required return periods. The flood frequency analysis predicted 150 m^3/s for the 50 year return period and 160 m^3/s for the 100 year return period, as visible from Figure 5.3, which will further be used for simulations in HEC-RAS. These values can be compared to a flooding study conducted on the Säveån, which gave 123 m^3/s for the 50 year return period and 135 m^3/s for the 100 year return period with today's climate, a difference that can be due to the deficit of data (Norconsult AB, 2015).

5.3 Water level as downstream boundary

There was no data for use as a downstream boundary of the study section i.e., where the Säveån river flows out to Göta Älv. Some analysis was done to find a representative value to use as water levels at this point, and a station at the Gothenburg harbor (Göteborg-Torshamn or GBGTOR) owned by the Swedish Meteorological and Hydrological Institute (SMHI) was used as a basis. The station is located at the downstream end of Göta Älv River and is a bit outside of the mouth of the river as seen in Figure 5.4. The station contained water levels at this point which were initially measured every hour, but in recent years were measured more frequent i.e. every 10 minutes and spanned from 1967 to 2012.

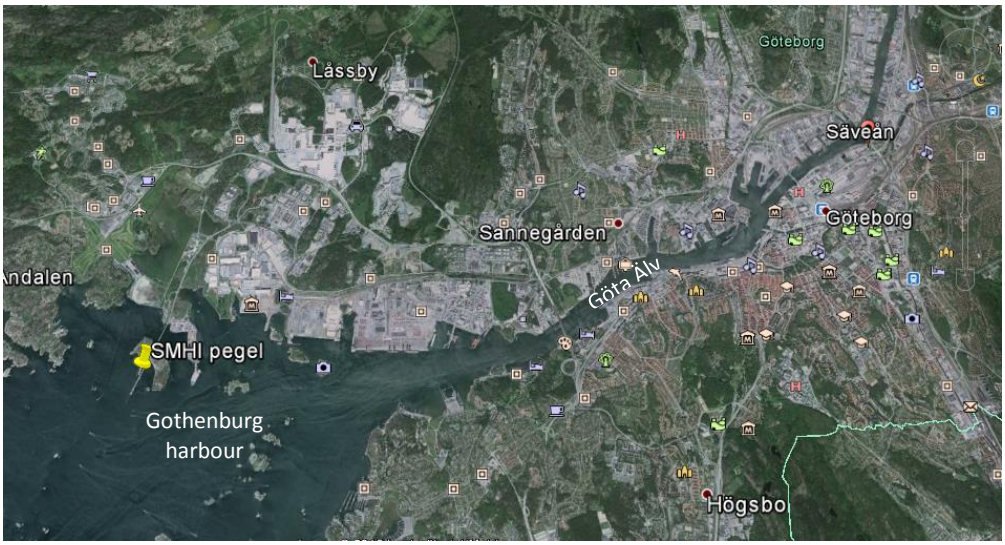

Figure 5.4: Google Earth view showing Göteborg-Torshamnen station (SMHI pegel) and downstream of Säveån, where the river joins with Göta Älv

A correlation was done between the flows from upstream of the study section of Säveån and the water levels at the Gothenburg harbor to find any dependencies between the two as seen in Figure 5.5. The time span for the water levels was matched with the available data from Säveån i.e. 2006 to 2010. It was found that the two variables produce a large scatter and little correlation with a low coefficient of determination. This concludes that the water level in the harbor and the flow from Säveån are independent variables and that the probabilities of a certain combined event may be obtained as the product of the probability of the individual events.

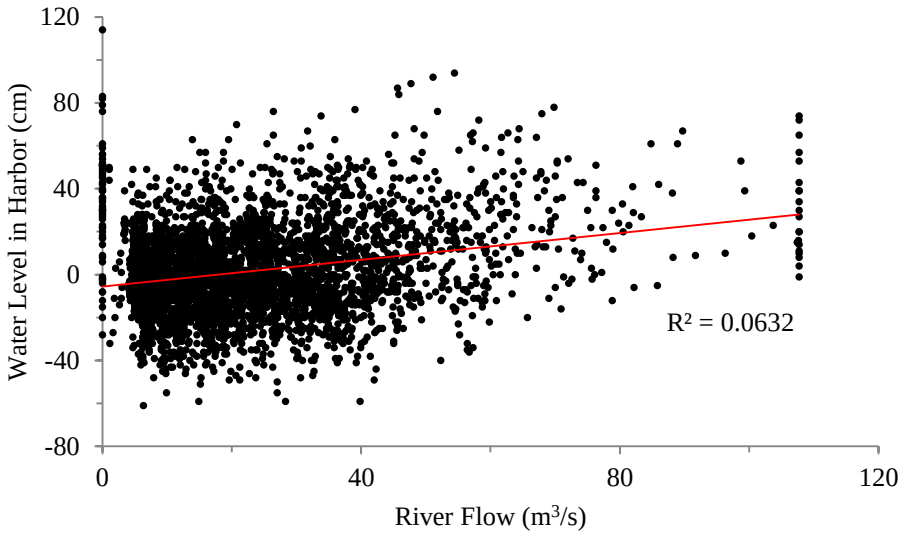

Figure 5.5: Water level in the harbor versus Säveån river flow for the period 2006 – 2010

It could be imagined that there would be some influence from Göta Älv, so that a large runoff from Säveån would be accompanied by a large runoff from Göta Älv, with higher water levels at the mouth of Säveån. But if there is any such effect, it is not seen by the GBGTOR data. Also water level at the GBGTOR is dependent on the westerlies that push sea water into the river. There are situations when the westerlies are combined with high river flows due to heavy rain.

Furthermore, the entire time series (hourly values) water level data from 1967 to 2012 for GBGTOR was analyzed in order to estimate the probability of specific water levels as seen in Figure 5.6.

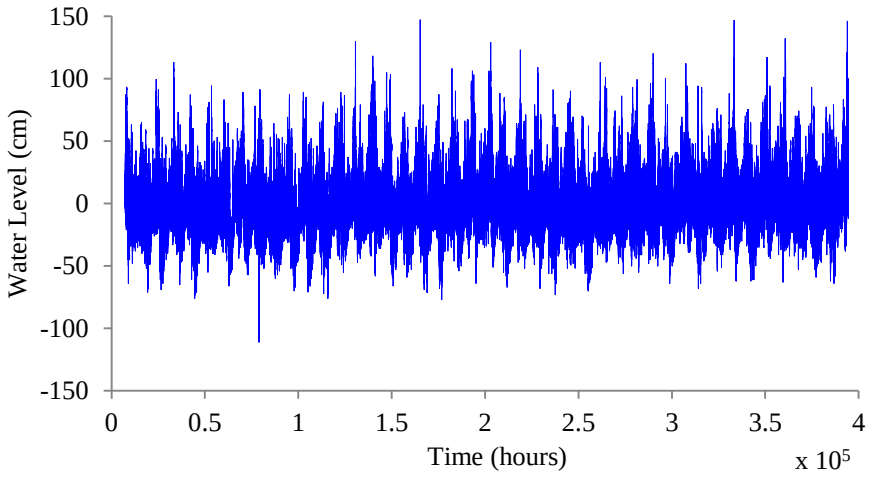

Figure 5.6: Water level time series for the GBTOR station for the whole time period of 1967-2012

The water levels refer to the mean sea level since the mean water level was subtracted from the series. The results reveal water levels of average 0 m but fluctuate between -0.5 m and 0.5 m. Säveån is located upstream and calculations indicate that on average the water level is 0.2 m higher at this point of exit to Göta Älv.

5.4 Schematization of river system

The study reach was divided into cross sections spaced 500 m apart starting upstream at just downstream of Jonsered hydropower station and ending at the outlet to Göta älv. The schematization was done in ArcGIS using the HEC-GeoRAS tool which extracts data for use with HEC-RAS. The upstream side of the river is characterized by meanders but gets straighter as it approaches downstream.

The river modeled section is about 13 kilometers and the river centerline is plotted using HEC-GeoRAS and a map of the area, starting from upstream at the downstream of Jonsered hydropower station to the outlet at Göta Älv. Cross sections are drawn and named with reference to the distance from the downstream, with upstream starting at cross section 13183.5 and last

downstream cross section at 206.9. The cross sections in-between are taken at 500 m intervals starting from cross section 13000 to cross section 500. The cross sections were further interpolated in HEC-RAS at intervals of 100 m, with an exception of river station 13000 to 12500 which is interpolated at intervals of 50 m for a more smooth transition of the bathymetry before simulations are carried out. The following figures (Figure 5.7 to Figure 5.14) shows the schematization of the river with photos of typical river section within the given reaches, starting upstream from river station 13183.5 to the downstream station 206.9.

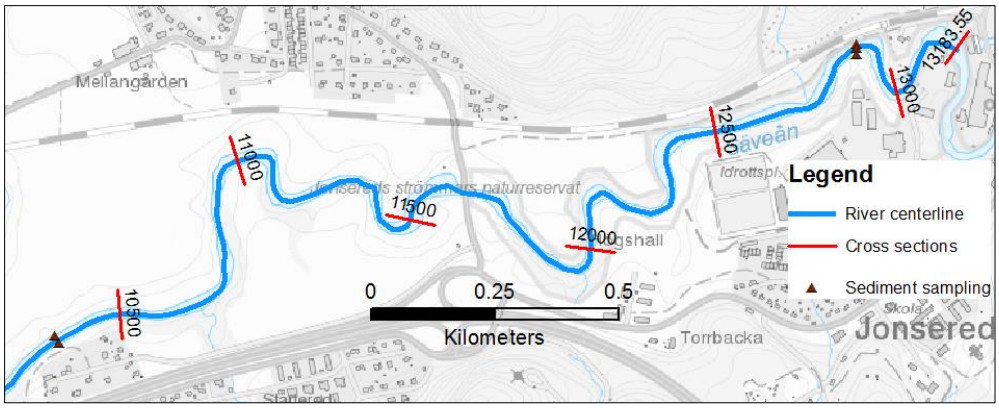

Figure 5.7: Säveån river study reach from section 13183.55 to section 10500. The brown spots show sediment sampling points

Figure 5.8: Typical river section at schematized cross section 11500 (Photo by Magnus Larson)

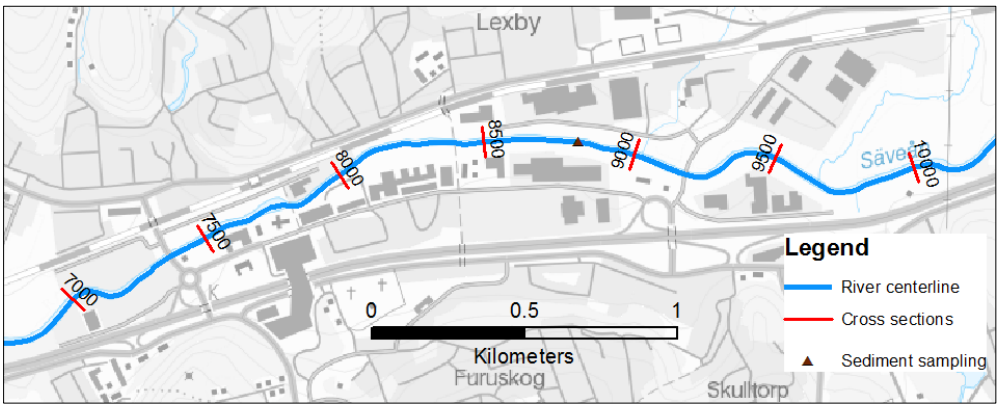

Figure 5.9: Säveån river study reach from section 10000 to section 7000. The brown spots show sediment sampling points

Figure 5.10: Typical river section at schematized cross section 9000 (Photo by Gasper Sechu)

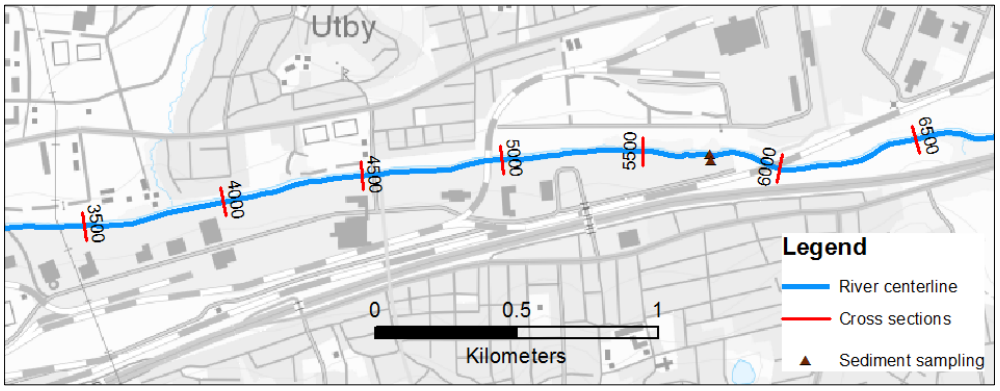

Figure 5.11: Säveån river study reach from section 6500 to section 3500. The brown spots show sediment sampling points

Figure 5.12: Typical river section at schematized cross section 4500 (Photo by Gasper Sechu)

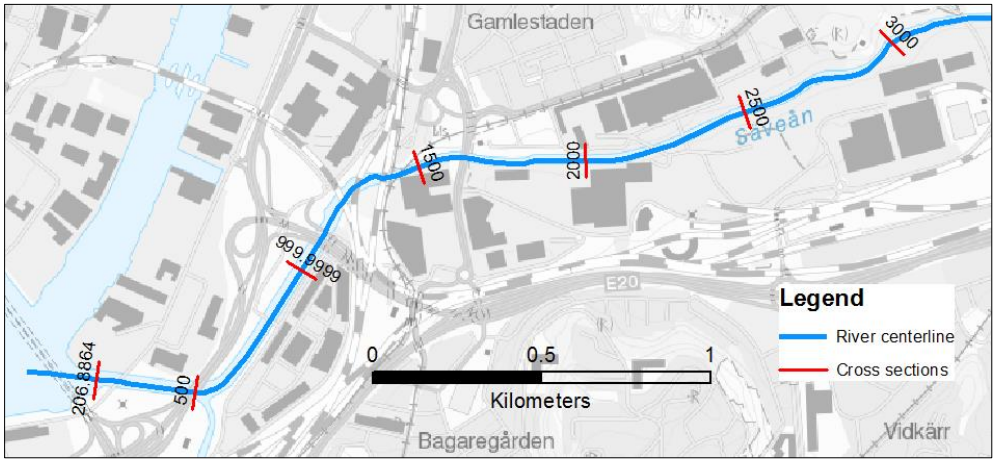

Figure 5.13: Säveån river study reach from section 3000 to section 206.9

Figure 5.14: Typical river section at schematized cross section 2500 (Photo by Gasper Sechu)

The river bed elevations start upstream at around 2.5 meters above sea level (msl) and increase to a maximum of about 3 msl at around cross section 12000. The elevations then gradually decrease to about -2.8 msl at the downstream end where the river discharges to Göta Älv. Figure 5.15 shows the longitudinal profile of the study area. The elevation data is for the year 2014 and is was collected by Clinton Mätkonsult AB, for SGI (Pedersen, et al., 2014).

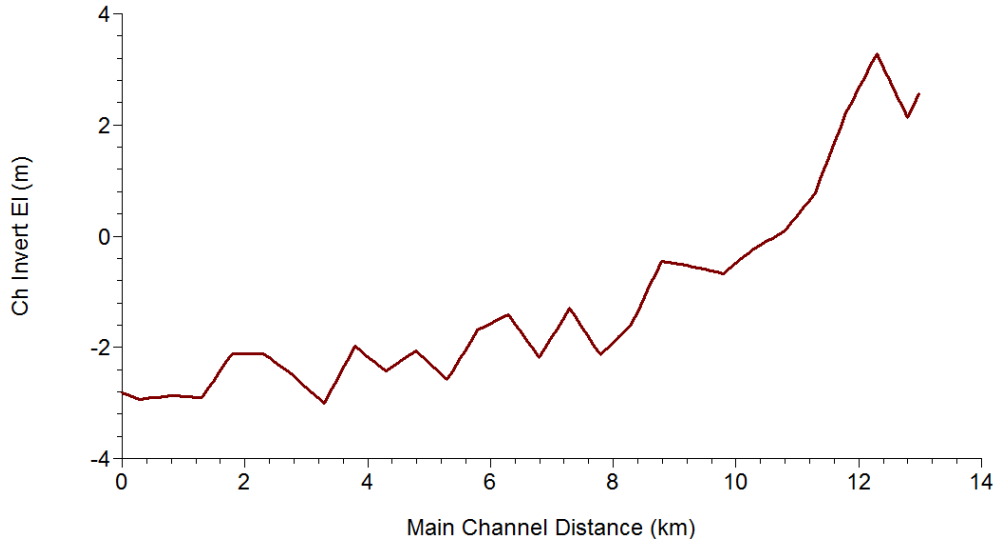

Figure 5.15: Channel bottom profile of the Säveån study section

5.5 Sediment data

Data was collected and analyzed for particle size distribution and the results were used for this study. The sediment is mostly fine with most grain sizes characterized between fine sand and clay. This is an important aspect in selecting the sediment transport function to use for the analysis as different functions were developed using grain size ranges. The grain size distributions for different sampling points are given in Table 5.2 adopted from HEC-RAS grouping of grain classes.

Table 5.2: Grain size distribution from sampling points within the study section

Grain classes	Grain diameter lower bound - upper bound (mm)	14CL014S	14CL0012S	14CL007S	14CL004S
Clay	0.002 – 0.004	1.4	2.4	2.8	6.5
Very fine silt	0.004 – 0.008	1.5	3.2	4.6	8.6
Fine silt	0.008 – 0.016	1.8	3.9	6.3	10.4
Medium silt	0.016 – 0.032	2.0	5.5	10.5	14.3
Coarse silt	0.032 – 0.0625	2.3	9.2	16.7	19.0
Very fine sand	0.0625 – 0.125	5.9	28.3	44.7	38.2
Fine sand	0.125 – 0.25	39.0	85.8	93.8	76.8
Medium sand	0.25 – 0.5	92.3	99.3	99.2	95.1
Coarse sand	0.5 - 1	98.9	99.7	99.6	97.0
Very coarse sand	1 - 2	99.4	99.9	99.9	98.1
Very fine gravel	2 - 4	99.9	100.0	100.0	98.8
Fine gravel	4 - 8	100.0	100.0	100.0	99.5
Medium gravel	8 - 16	100.0	100.0	100.0	100.0
Coarse gravel	16 - 32	100.0	100.0	100.0	100.0
Very coarse gravel	32 - 64	100.0	100.0	100.0	100.0

Four sampling points for sediment data within the study reach; 14CL014S, 14CL012S, 14CL007S and 14CL004S were used in the simulations. These sampling points are located just downstream of cross sections 13000, 10500, 9000 and 6000 respectively as shown in schematization diagrams in Figure 5.7, Figure 5.9 and Figure 5.11. The grain size distribution graphs are given in Figure 5.16.

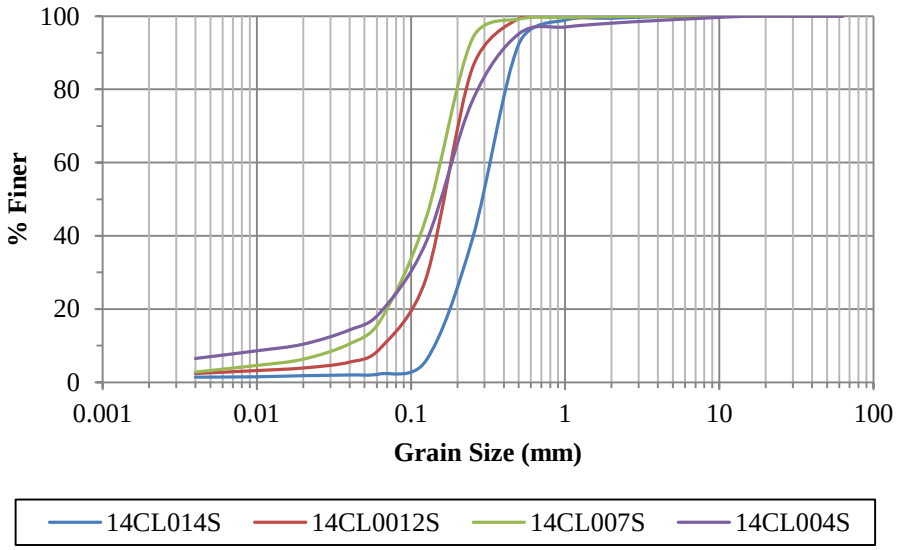

Figure 5.16: Grain size distribution for the sediment data used in the study

6 Model simulations

Prior to model simulations model setup was done. This included exporting cross sectional bed data from HEC-GeoRAS to HEC-RAS. Two simulation capabilities were used in HEC-RAS and these are steady flow simulation and sediment transport simulation. With steady flow simulation, geometry data (cross sectional bed data) and steady flow data is used. Sediment transport simulations required geometry data, quasi-unsteady flow data and sediment data. Quasi-unsteady flow is essentially discharge at given intervals and therefore the time series flow data for Säveån was used. Erosion and bank stability studies were simulated using the model SLOPE/W.

The simulations started with a series of hydrodynamic flow simulations using mean river flow for the study section. This was performed using steady flow simulation function in HEC-RAS. The results enabled sensitivity and extreme event analyses of the study section. This was followed by sediment transport simulations of the study reach. The results were analyzed to quantify the sediment transport along the river. Furthermore, results from the sediment transport simulations were used as input to SLOPE/W. They were used to assess and quantify the effect that sediment transport has on river bank stability. Finally, some further simulations were carried out by HEC-RAS to determine some climate change effects on the sediment transport.

For an initial hydrodynamic simulation run with the mean river flow 24 m^3/s, some hydraulic parameters i.e. the water surface elevation, channel velocity and total shear stresses are plotted (Figure 6.1 to Figure 6.3 respectively) for the study section.

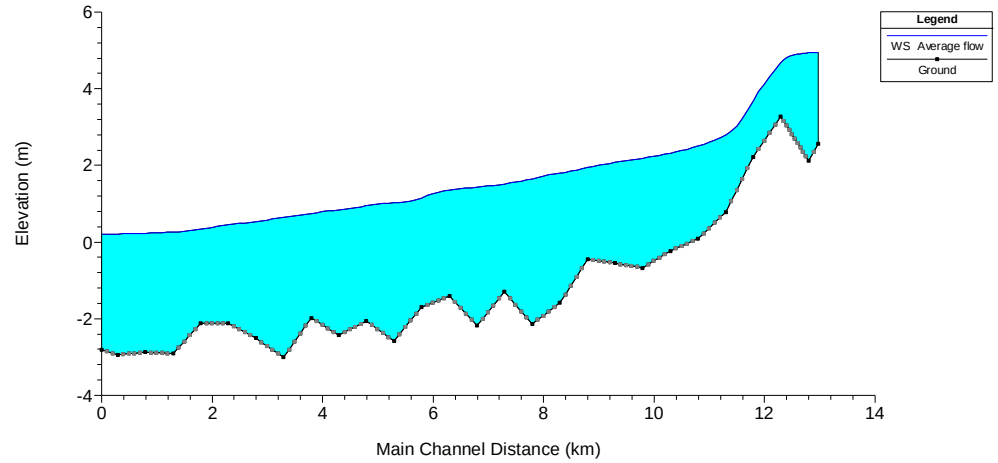

Figure 6.1: Water surface elevations throughout the study section for mean flow simulation

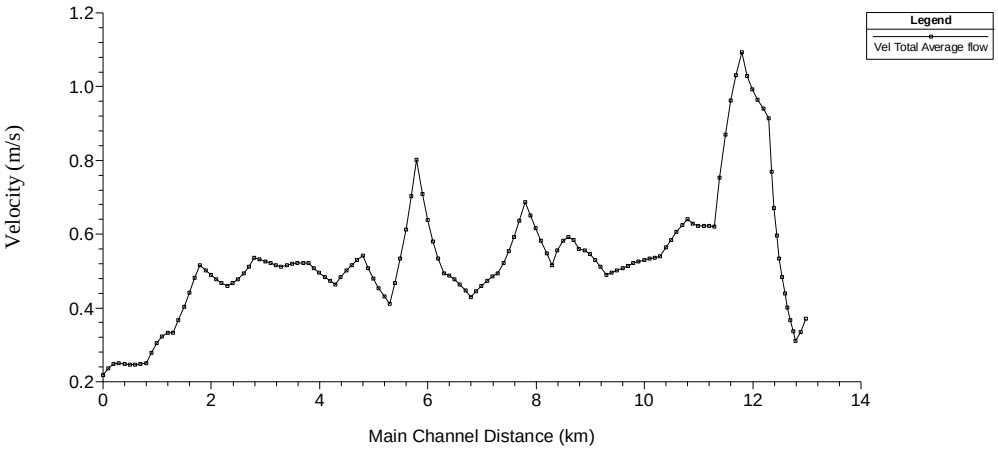

Figure 6.2: Average channel velocity throughout the study section for the mean flow simulation

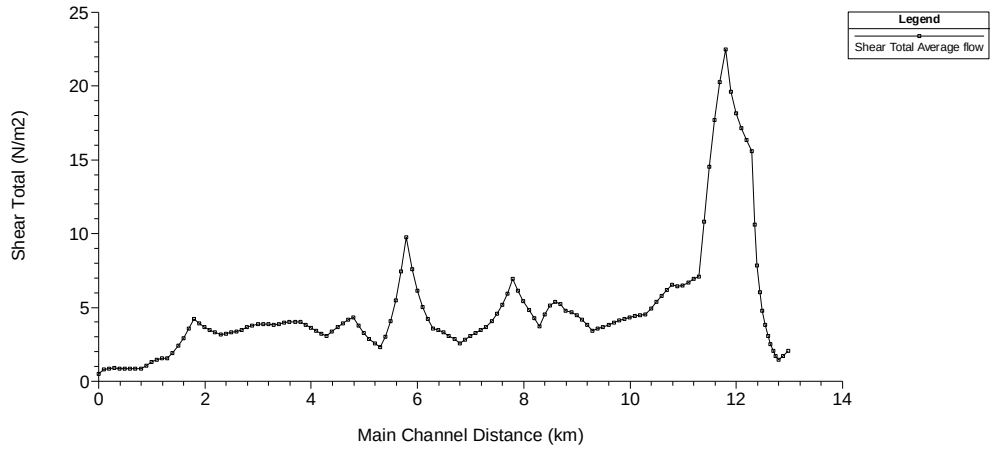

Figure 6.3: Average bed shear stress throughout the study section for the mean flow simulation

At the upstream end, the simulated water surface elevation is at about 4.95 msl and decreases gradually to a downstream water level of 0.2 msl. A sharp decrease in the water level occurs roughly between cross section 12500 and 12000, and this is due to the rise in the bed elevation from cross section 12500 to cross section 12000. The highest channel velocity, 1.1 m/s occurs at around cross section 12000 and the lowest, 0.2 m/s occurs at the most downstream cross section. Likewise, the highest shear stress, 22.5 N/m^2 occurs around cross section 12000 and the lowest, 0.5 N/m^2 occurs at the most downstream cross section.

6.1 Sensitivity analysis

Since the water levels at the downstream end of the study reach are uncertain, a sensitivity analysis was carried out to test how the model performs with variation of the downstream water levels, where the Säveån meets Göta Älv. Steady flow simulations were carried out for the average flow between the applied flow data of 2006 to 2010 which came up to 24 m^3/s and the downstream boundary condition varied. Steady flow simulations using subcritical flow conditions do not require an upstream boundary in HEC-RAS. To assess the sensitivity of the model due to the uncertainty in the downstream water level, the variation in the total shear stress along the study reach was used since it is the parameter of interest when it comes to sediment transport. Simulations were done for downstream water levels of 0.2 m which

is taken as a representative level, and water levels 0.5m above and below 0.2 m i.e. 0.7 m and -0.3 m respectively as given in Figure 6.4.

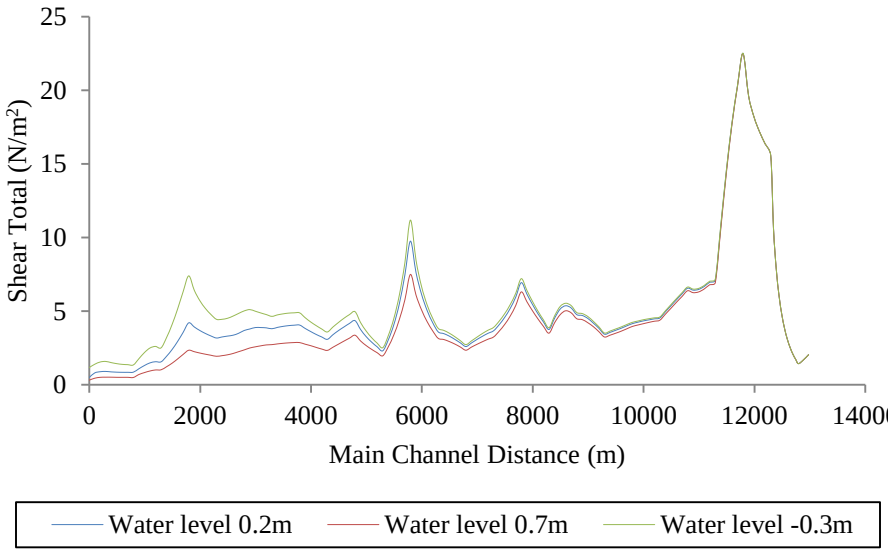

Figure 6.4: Total shear shear stess variation throughout the river reach as a result of varying the downstream water level

From Figure 6.4 it can be drawn that the shear stress variation due to the change in downstream water levels gets more pronounced downstream of the river reach. Also the shear stress decreases as a result of increasing the downstream water level and vice versa. The changes in the shear stresses are however significant with the most pronounced change at around river station 2000, where the shear stress is around 4 N/m^2 for 0.2 m downstream water level, 2 N/m^2 and 7 N/m^2 for 0.7 m and -0.3 m downstream water levels respectively. But the changes are rather small at the point of interest, which is the upstream side of the river reach. Due to this, the downstream water level of 0.2 m is therefore used as a constant boundary condition for the sediment transport simulations that follow.

6.2 Flows and water levels during extreme events

HEC-RAS steady flow simulations were done for the average flow of 24 m^3/s, 50 year return flow of 150 m^3/s and 100 year return flow of 160 m^3/s. The

downstream boundary condition is established as 0.2 m. The water surface profiles as a result of the simulations are given in Figure 6.5.

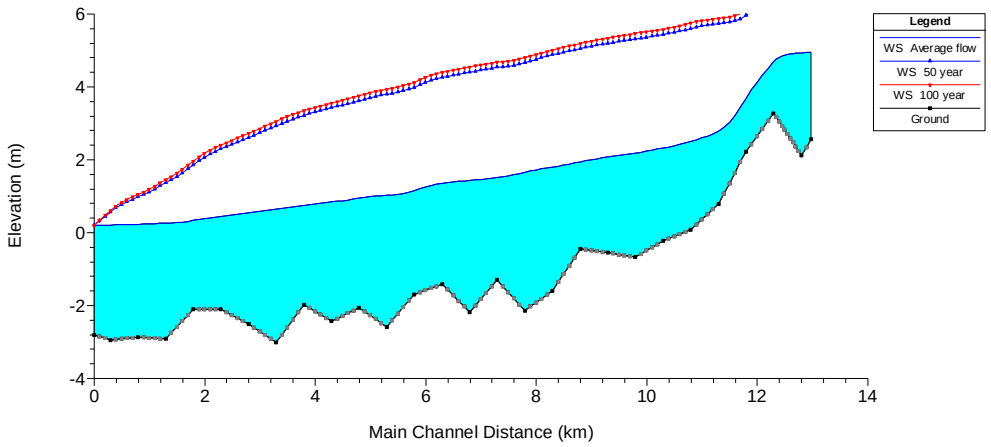

Figure 6.5: Water surface elevation from steady flow simulations showing the average flow and extreme events simulations

The water surface profile rises significantly as a result of 50 and 100 year return flow simulations. The water surface elevations in each cross section are given in Appendix 1 for better visualization. The significant rise in the water surface elevation due to the return floods leads to a high risk of flooding as seen for example in cross section 7500 in Appendix 1.

6.3 Sediment transport and erosion during extreme events

Sediment transport was also simulated for the extreme flooding events. Figure 6.6 gives the total shear stress variation results from HEC-RAS simulations for the steady flow simulations with average flow, 50 year return flood and 100 year return flood profiles.

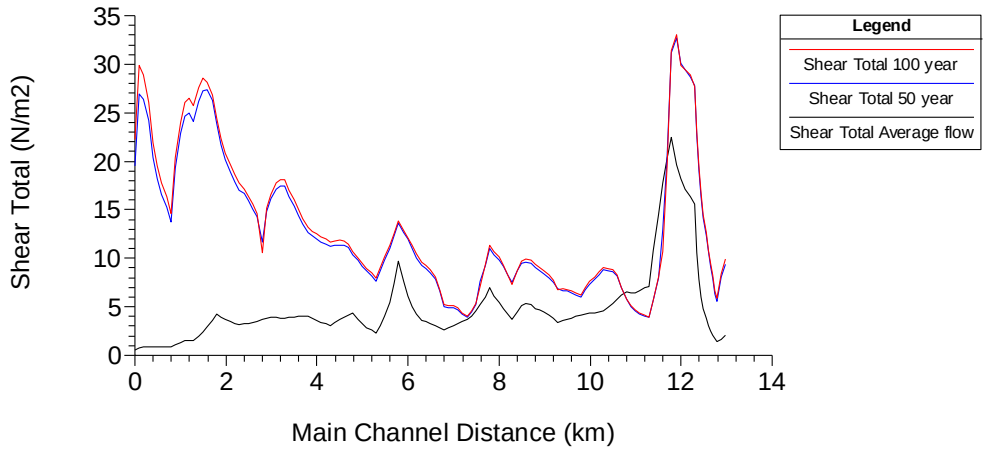

Figure 6.6: Steady flow simulation showing the total shear stress variation as a result of the average flow and extreme events simulations

The results reveal a substantial increase in the shear stress throughout the study reach due to simulations of the two extreme events. This in turn comes with more erosive capability as a result of sediment transport.

A sediment transport, mobile bed computation simulation is also done for extreme events, and the results given in Figure 6.7.

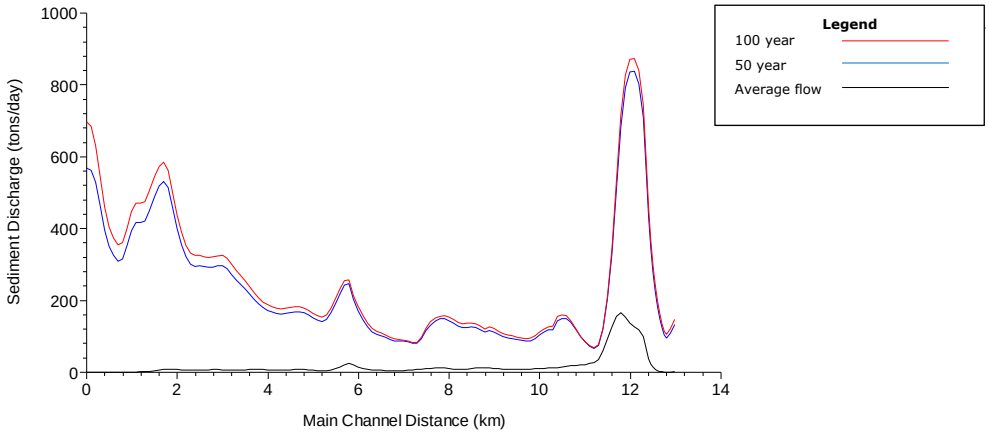

Figure 6.7: Sediment spatial plot showing the variation of sediment discharge for the extreme events in comparison to the average flow

The results from Figure 6.7 show a significant increase in the sediment load due to the simulation of the extreme events. Taking the most extreme erosive

river station at 12500, the simulation predicts sediment loads of 160 tons/day for the average flow, 840 tons/day for the 50 year return flood and 880 tons/day for the 100 year return flood.

6.4 Annual sediment transport along the river

Annual sediment transport can be taken as the amount of sediment that leaves the study reach within a year. By studying the HEC-RAS sediment transport results from the most downstream river section in the model schematization i.e. station 206.9, the time series trend for the sediment discharge gives the sediment load leaving the river in time. Figure 6.8 gives the sediment discharge in tons/day time series at the downstream river station 206.9 where the Säveån meets Göta Älv, which is then the rate out from Säveån to Göta Älv. Additionally, in order to study the amount of sediment that has eroded or deposited within the river in time, the sediment discharge rate at the upstream river station 13183.5 is also given in Figure 6.9.

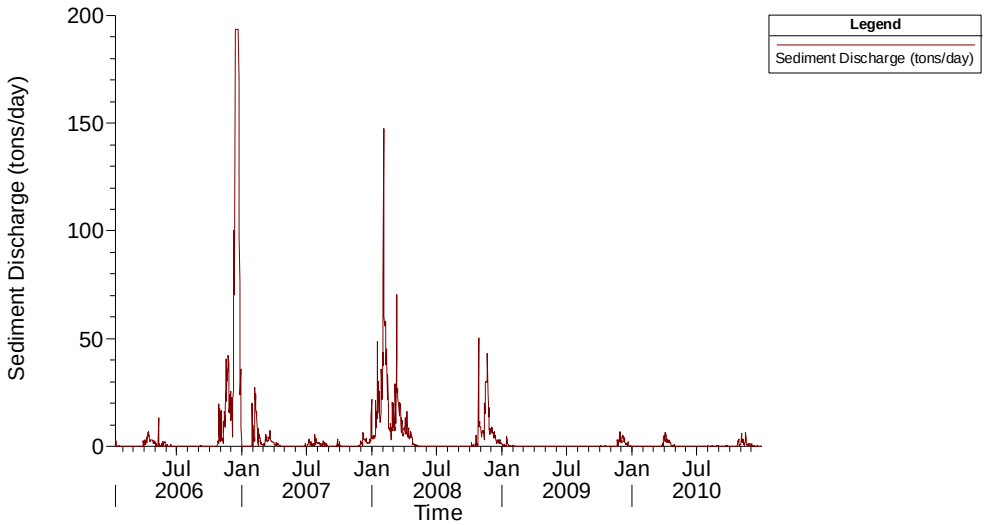

Figure 6.8: Sediment discharge time series taken at the most downstream river section 206.9 for the simulation period 2006-2010

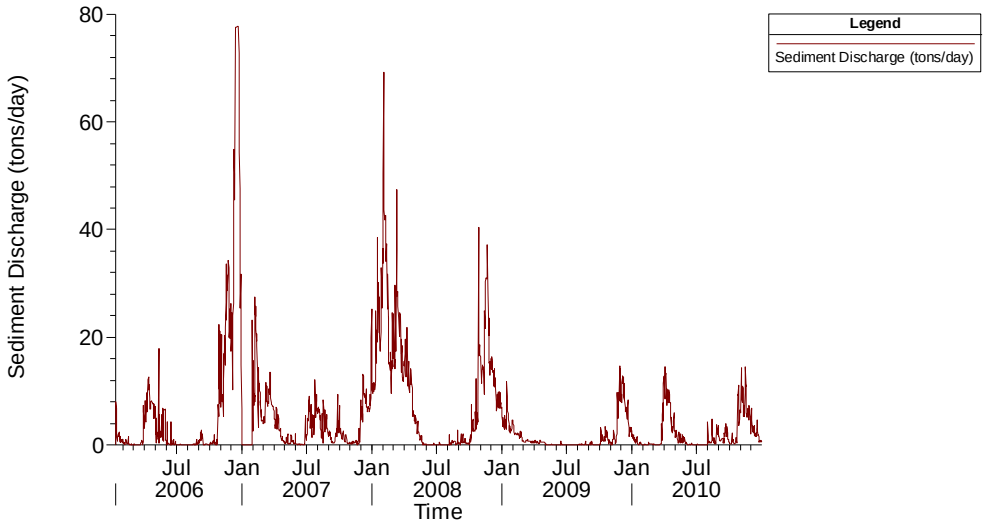

Figure 6.9: Sediment discharge time series taken at the most upstream river section 13183.55 for the simulation period 2006-2010

From Figure 6.8, the sediment discharge leaving the river varies from season to season depending on the flows and the trend can be compared to the time series flow data applied at the upstream boundary given in Figure 5.1. Sediment discharge peak values occur in time where there are also peak flows according to the flow data applied. The biggest sediment load occurs around December 2006 at around 190 tons/day and around February 2008 with 150 tons/day, with the times being in line with the flow time series peaks.

In order to analyze the total sediment transport during the years, the daily sediment load discharge at the downstream river station 206.9 (Figure 6.8) are cumulated yearly as given in Figure 6.10.

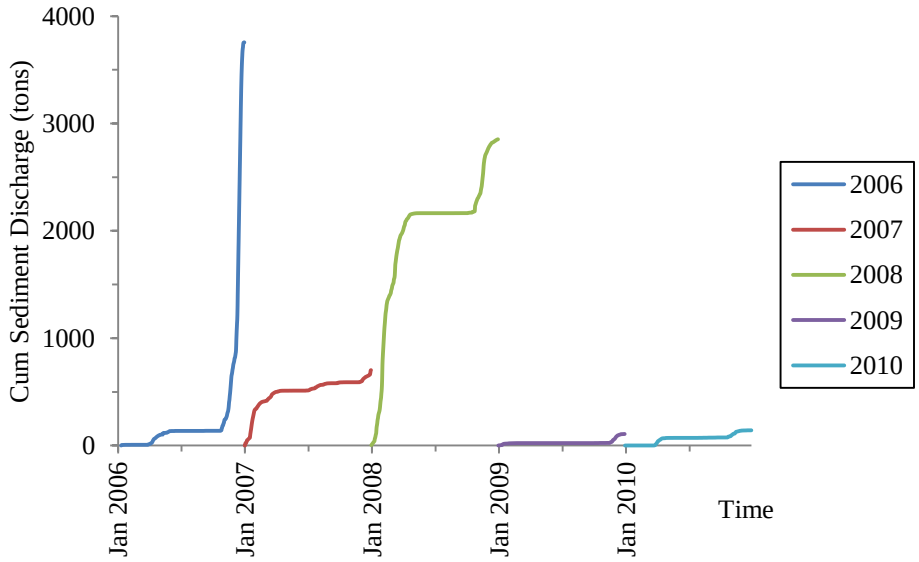

Figure 6.10: Cumulative sediment discharge time series in tons taken at the most downstream river section 206.9, for the simulation period 2006-2010

The results for annual sediment discharge vary from year to year as seen in Figure 6.10. The observed values are 3,750 tons/year, 700 tons/year, 2,850 tons/year, 100 tons/year and 140 tons/year for years 2006, 2007, 2008, 2009 and 2010 respectively. Table 6.1 compares the annual sediment transport with the mean and maximum flows for each of the simulation years. It is observed that years with high maximum flows correspond with large values of the sediment transport, the highest being the flooding year of 2006 which had the highest annual sediment transport of 3,750 tons.

Table 6.1: Annual sediment transport and corresponding mean and maximum flows

Year	**Sediment transport (tons/year)**	**Mean flow (m^3/s)**	**Max flow (m^3/s)**
2006	3,750	27	108
2007	700	27	63
2008	2,850	33	99
2009	100	16	51
2010	140	19	56

Furthermore, cumulating the annual differences between the sediment discharge of the most downstream cross section (which is the sediment load

leaving the river) and the most upstream cross section (which is the sediment load entering the river), the results give the net annual sediment budget for the simulation years as seen in Figure 6.11 below.

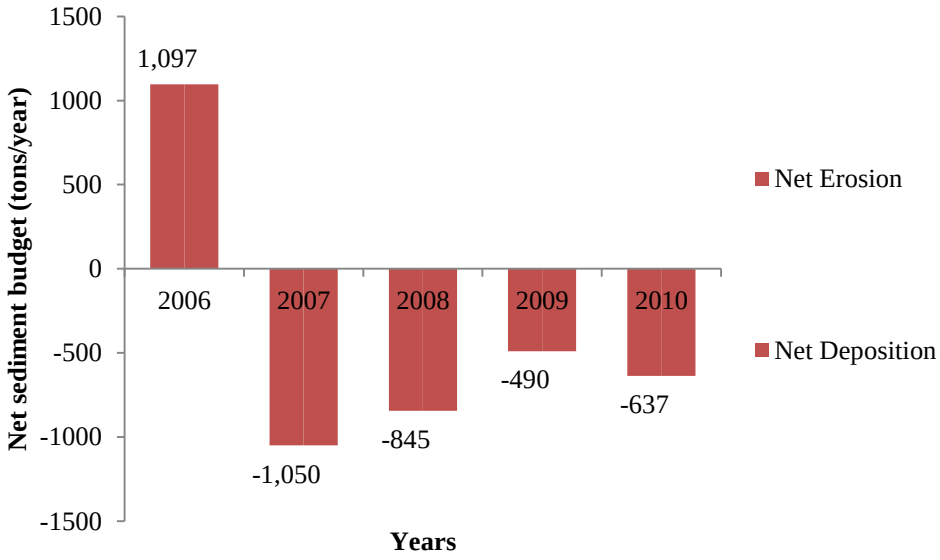

Figure 6.11: Net annual sediment budget for the Säveån study section

The results reveal that only the year 2006 has net annual sediment erosion of 1,097 tons with the rest of the years having net annual sediment deposition as seen in Figure 6.11. The reason for this can also be related to the flooding event in the simulation year 2006 which gave rise to high amounts of sediment discharge compared to the subsequent simulation years.

6.5 River stretches sensitive to long-term erosion

Furthermore, river stretches that are sensitive to long-term erosion are analyzed as a prelude to finding sections to analyze for slope failure. HEC-RAS sediment spatial plot is used to visualize the channel invert variation in time (Figure 6.12) and the cumulative mass bed change in time (Figure 6.13) as a result of sediment transport simulations. The channel invert is investigated after every one simulation year, starting from the start of the simulation 2006-01-10 to the end at 2010-12-31.

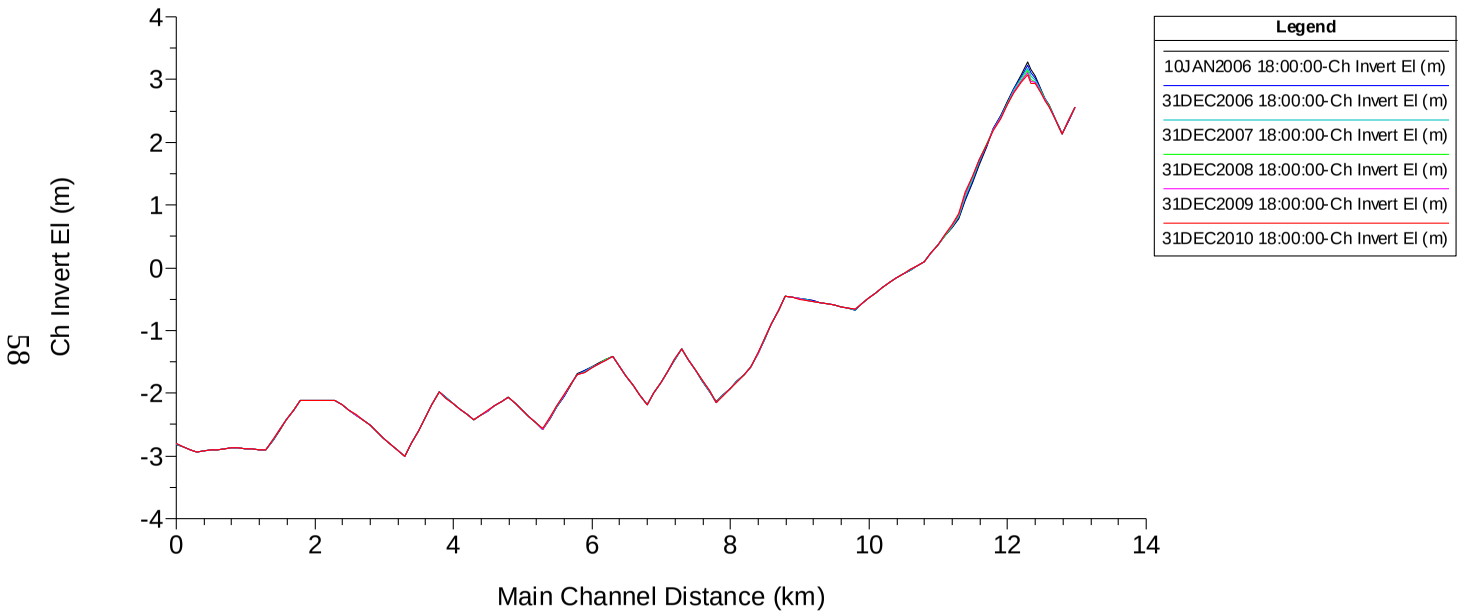

Figure 6.12: Sediment spatial plot showing the variation of the channel invert in time

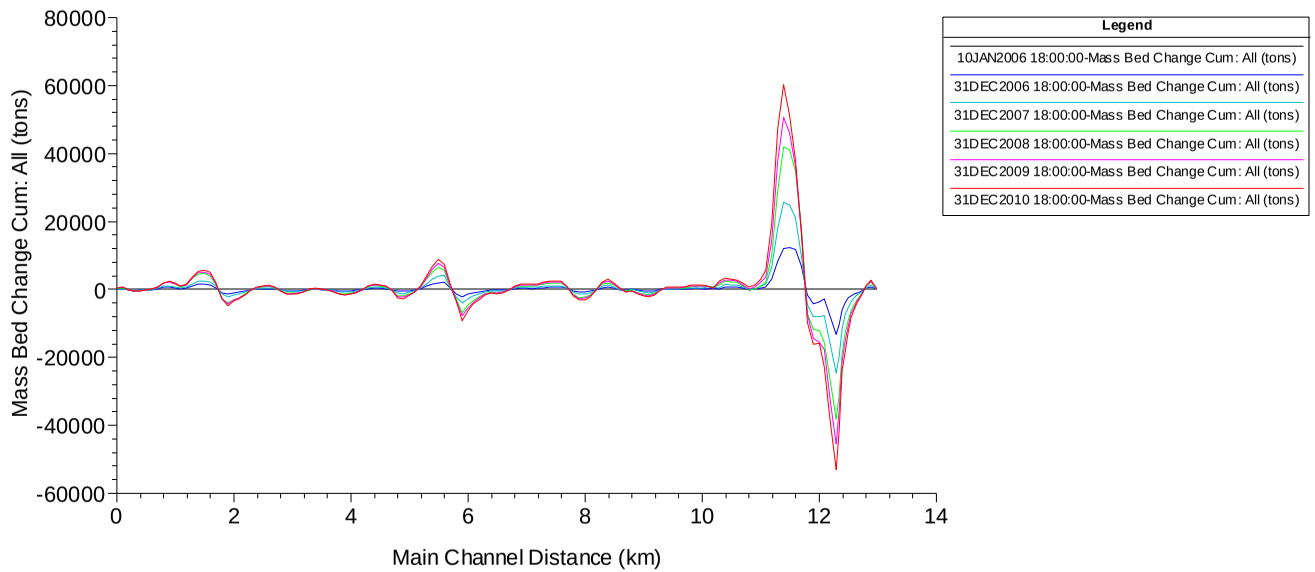

Figure 6.13: Sediment spatial plot showing the cumulative mass bed change with time

The observed channel inverts reveal that the river section 12500 has the most progressive erosion trend. For visualization of the erosional changes in the station 12500, Figure 6.14 gives the cross sectional bed changes in time. The bathymetric changes are given yearly from start of simulation 2006-01-10 to 2010-12-31. For a better view of the bed changes in time, Figure 6.15 shows the river channel magnification derived from Figure 6.14.

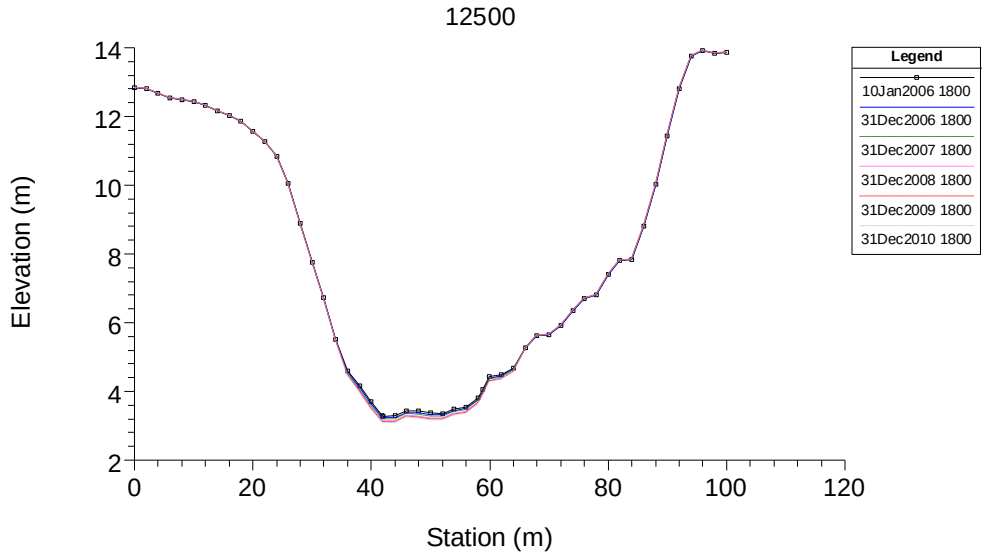

Figure 6.14: Cross section of the river station 12500 showing the change in the bathymetry due to erosion

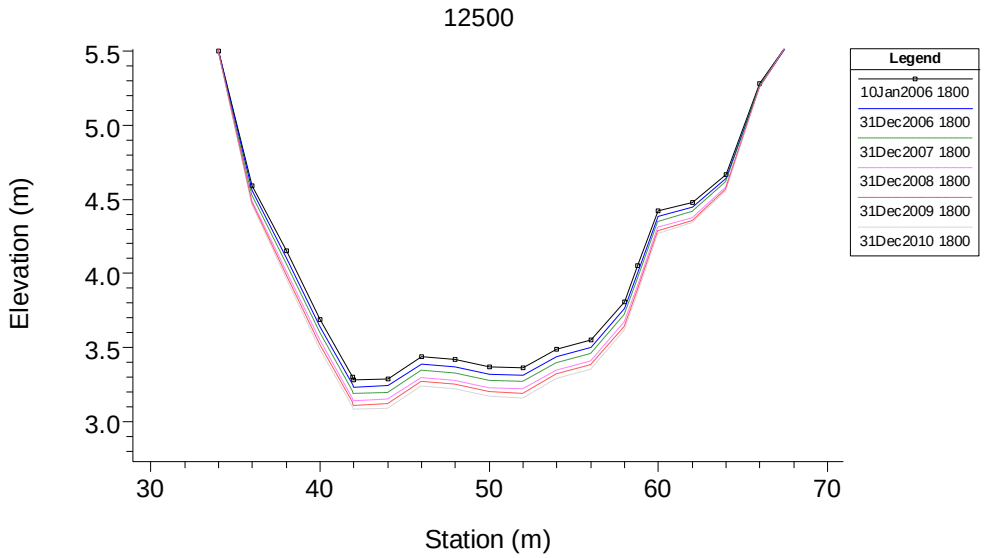

Figure 6.15: Magnification of the river channel at cross section 12500

The section is further analyzed using a time series to find the amount of mass that has eroded in time as seen in Figure 6.16.

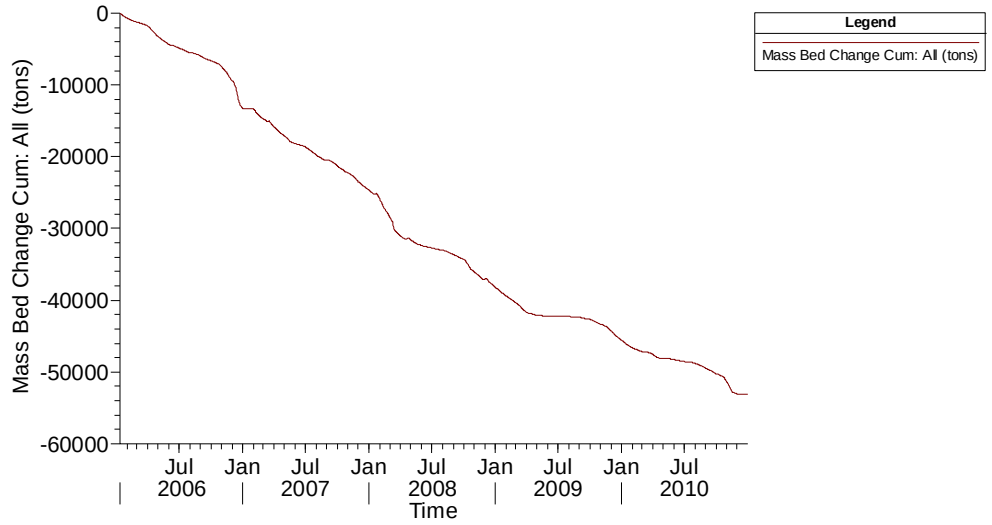

Figure 6.16: Sediment time series showing the variation of the cumulative mass bed change for the river section 12500

The sediment time series shows that the river section 12500 erodes continuously in a linear nature throughout the simulation years. The negative

sign in the curve shows that the section is eroding. The cumulative eroded mass at this section accumulates to around 53000 tons. Note that some of this eroded mass will be accreted at further downstream river stations but the focus of this project is on the eroding sections.

6.6 Implications of erosion for bank stability and slope failure

The implications of the erosion to the river bank stability will be analyzed for the most eroded river station i.e. 12500. This section is analyzed as an example and the other eroding sections may be evaluated as needed. The results from HEC-RAS are used as a basis, and the model GeoStudio is used for the analysis of the slope failure. GeoStudio is geotechnical modelling software with various products, and the specific product that can analyze slope stability is the SLOPE/W.

SLOPE/W has a lot of options but for simpler understanding of its capacity, it can be divided into five components which have been classified to help understand the model while formulating a problem (GEO-SLOPE International Ltd, 2012). These include:

- Geometry – this provides the depiction of the shape and stratigraphy of the potential slip surface.
- Soil strength – these are factors used to describe the soil material strength.
- Pore-water pressure – this gives the possibility to describe the pore-water pressure conditions in the soil.
- Reinforcement or soil-structure interaction – these include anchor elements such as nails, piles, walls, fabric and so forth that may be included in the model.
- Imposed loading – includes anything superimposed such as a surcharge load or an earthquake loading.

The model uses the method of slices which dissects the slip surface into a number of slices and during simulation it balances forces acting on every individual slice (GEO-SLOPE International Ltd, 2012) as seen in Figure 6.17.

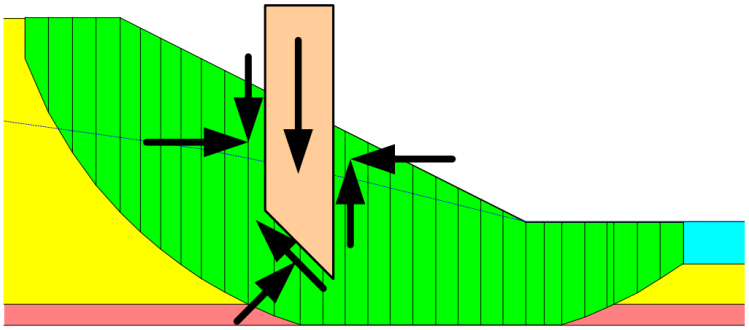

Figure 6.17: SLOPE/W model setup showing dissection of the slip surface into slices and balance of forces on a slice

The bank stability is analyzed using yearly cross sectional bathymetric changes due to erosion caused by sediment transport. Six simulations are conducted for the left bank of station 12500, starting with the initial bathymetry taken with flow data for 2006-01-10 (Figure 6.18). The bank stability is simulated using the bathymetric changes observed at the end of the years 2006, 2007, 2008, 2009 and 2010 respectively. The safety factor for failure is used as a basis to quantify the yearly loss in stability due to erosion.

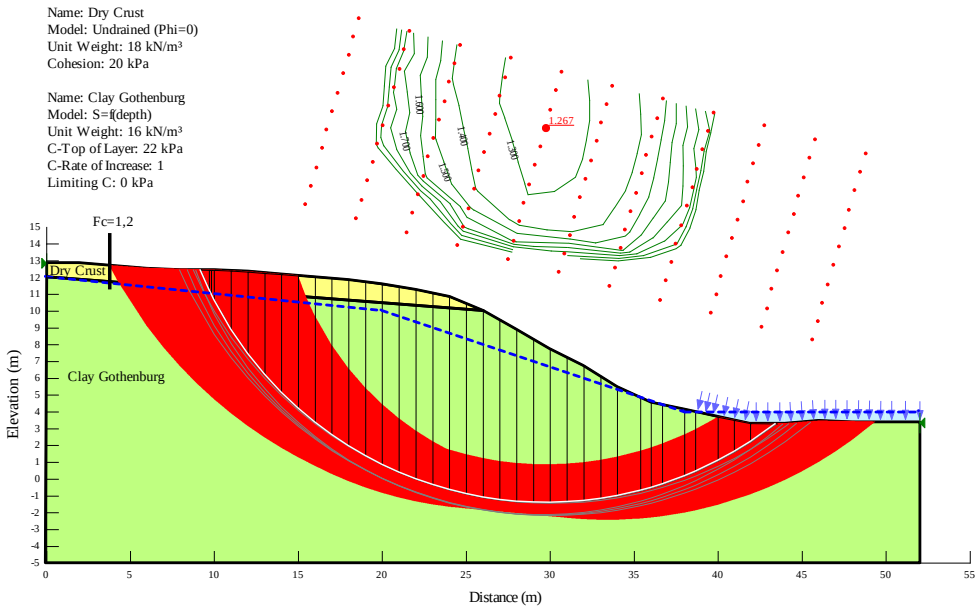

Figure 6.18: Results from SLOPE/W showing the analysis of the slope stability for the base time 2006-01-10 with given safety factor

The safety factor at the start of simulations is 1.267 as seen in Figure 6.18. Also the red area in the figure indicates the safety map, under which slip surfaces with similar factors of safety could develop. The analysis for the other years is given in Appendix 2. Table 6.2 gives the factors of safety as observed from the analysis of bank stability.

Table 6.2: Factors of safety observed from analysis of the bank stability using SLOPE/W

Time	**Factor of Safety**
2006-01-10	1.267
2006-12-31	1.263
2007-12-31	1.26
2008-12-31	1.256
2009-12-31	1.254
2010-12-31	1.252

From the results, it can be drawn that, the factor of safety reduces on average 0.003 every year due to erosion caused by sediment transport. If the rate of erosion persists, it could lead to safety factors below 1.0 in about 89 years (2095) from the beginning of the simulation (2006) which may then result in bank failure.

6.7 Climate change effects

Climate change is becoming a major concern in studies of the natural systems. So much uncertainty comes with climate change and most studies only give estimations of scenarios that may or may not occur. In this study, the interest lies on the effect of climate change to the flow and sediment transport in the Säveån. The data was extracted from a study done by SMHI on climate changes analysis (Persson, et al., 2011). Figure 6.19 shows river flow data as a result of climate change simulation scenarios. The data consists of plotted flow simulations for the period 2021-2050 that was a result of 16 climate scenarios and simulation period 2069-2098 that was a result of 12 climate scenarios and these are compared to a reference period of 1963-1992.

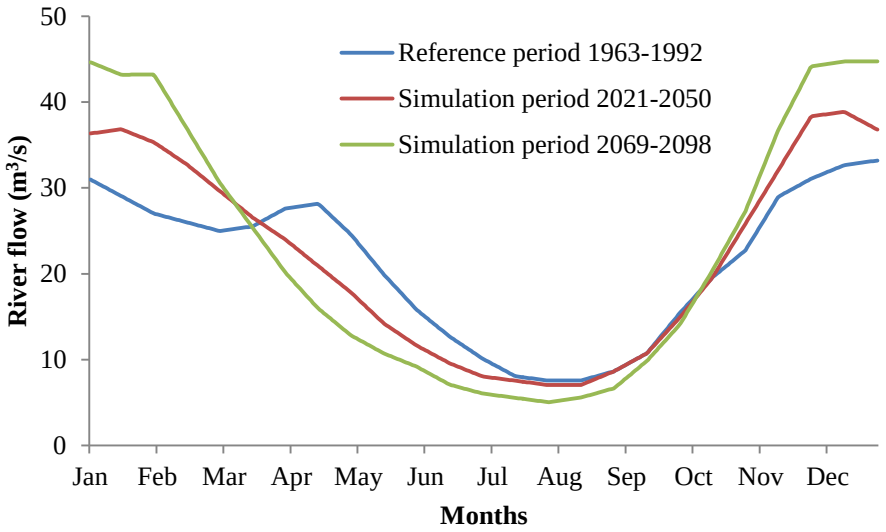

Figure 6.19: Säveån river change in the seasonal dynamics of the total inflow for the period 2021-2050 and the period 2069-2098 compared to the reference period 1963-1992 (Persson, et al., 2011)

The data was subjected to a one year simulation in HEC-RAS to compute the amount of sediment transport that would occur for the two climate simulation periods as compared to the established reference period (Figure 6.20).

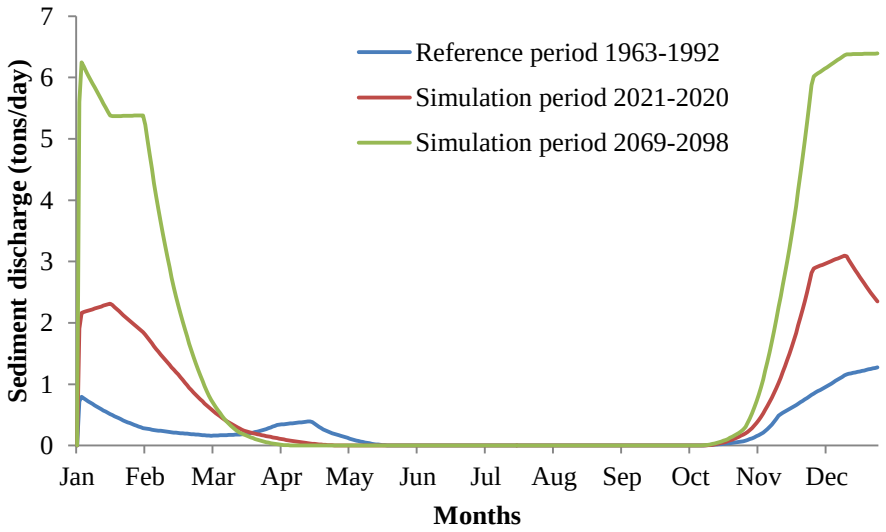

Figure 6.20: Sediment discharge at the downstream cross section 206.9 due to simulation of the climate change scenarios and reference period

The results reveal higher sediment discharge with simulation of climate change scenarios as compared to the reference period. The annual sediment discharge from the river comes up to 86 tons, 233 tons and 522 tons for the reference, 2021-2020 and 2069-2098 simulation periods respectively. This concludes that climate change is accompanied with higher flows and sediment transport respectively.

7 Discussion

The HEC-RAS hydrodynamic simulations for the extreme events reveal a significant rise in the water level within the study reach. The 3 to 4 meter rise in the water level can be interpreted as a sign of flooding and inundation. Flooding protection measures are required to overcome catastrophes that come with these events and further studies on costs associated with these are highly recommended.

The sediment transport simulations on the other hand reveal an irregular pattern in the yearly annual sediment budget leaving the study section. The biggest sediment discharge occurred in 2006 with about 3750 tons/year of sediment leaving the river. This is the same year that had the highest flows due to flooding that occurred in December. These results should however be taken with caution due to lack of sediment discharge observations for calibration and validation of the model. It is therefore recommended as an aid for future studies, that more gauging stations are added to the river reach and that sediment load data be prioritized along with flow and stage data. Furthermore, apart from simulation year 2006 which gave net annual erosion, all the other subsequent simulation years revealed a net annual deposition. Net deposition does not necessarily mean that the river does not erode, but could also be that some areas are eroding sediments and depositing before they leave the river.

One river station was found to be eroding at a faster rate than the others, i.e. station 12500 and was therefore used an example for slope stability. The bank slope analysis from SLOPE/W gave an average yearly loss in the factor of safety of about 0.003 for the left bank. This value is theoretical and should be used as an initial estimate only. It is suggested that this station is given a more detailed geotechnical study, which should go hand in hand with suggestions for stabilization.

And finally, the climate scenario simulations show an increasing amount of sediment transport in the river with climate change. With increasing river flows, sediment discharge is bound to increase and this will most likely lead to erosion and bank stability problems within Säveån.

Conclusions

The focus of the report was to estimate the transport of sediment within the Säveån and extend this to find its implications on erosion and bank stability. The scope extended to find some climate change effects on the flow and sediment transport within the river.

The approach was the use of ArcGIS in combination with Hec-GeoRAS to map out the river and extract cross sections from a Digital Elevation Model (DEM) of the river. HEC-RAS was then used for the simulation of the river steady flow modeling and sediment transport mobile bed computations. The river flow data was available for years 2006 to 2010 and bathymetry data was for the year 2014. HEC-RAS satisfactorily simulated the flows and water levels for the average flow and extreme flows within the study river reach.

Sediment transport simulations showed schematized river section 12500 as the most erosive river section and further slope stability analysis were done at this location as an example. The simulations for the slope stability were carried out using the model SLOPE/W. The estimated yearly loss in factor safety of 0.003 for the left river bank at this point suggests that the bank will collapse within about 89 years from the beginning of the simulation.

With climate change, simulations were done using flow data obtained from climate scenarios for the years 2021-2050 and the years 2069-2098. These were compared with data from a reference climate period 1963-1992. The results suggest an increase with sediment discharge of more than half from the reference period to the climate period 2021-2050 and again more than double the increase from time period 2021-2050 towards the end of the century.

Finally, as a recommendation, it could be of great value that Swedish rivers including the Säveån be equipped with measurements of sediment loads to ease the calibration process in estimation of sediment transport.

References

Ackerman, C. T., 2012. *HEC-GeoRAS, GIS Tools for Support of HEC-RAS using ArcGIS, User's Manual,* California: US Army Corps of Engineers.

Ackers, P. & White, W. R., 1973. Sediment Transport: New Approach and Analysis. *Journal of the Hydraulics Division, American Society of Civil Engineers,* 99(11), pp. 2040-2060.

Bogardi, J., 1968. *Incipient Sediment Motion in Terms of Critical Mean Velocity,* s.l.: Acta Tech. (Budapest) 62, 1.

Brandt, M., 1990. Generation, Transport and Deposition of Suspended and Dissolved Material - Examples from Swedish Rivers. *Geografiska Annaler. Series A, Physical Geography, Vol. 72, No. 3/4,* pp. pp. 273-283.

Brunner, G. W., 2010. *HEC-RAS, River Analysis System User's Manual, Version 4.1 Report CPD-68,* California: US Army Corps of Engineers.

Camenen, B. & Larson, M., 2007. *A Unified Sediment Transport Formulation for Coastal Inlet Application,* Washington, DC: U.S. Army Corps of Engineers.

Chaudhry, M. H., 2008. *Open-Channel Flow.* 2nd ed. Columbia: Springer Science & Business Media, LLC.

Copeland, R. R. & Thomas, W. A., 1989. *Corte Madera Creek Sedimentation Study,* s.l.: Numerical Model Investigation. US Army Engineer Waterways Experiment Station, Vicksburg, MS. TR-HL-89-6.

Engdahl, M. & Påse, T., 2014. *Geologisk beskrivning av Säveåns dalgång, SGU-rapport 2014:37 (Swedish),* Uppsala: Sveriges geologiska undersökning.

Engelund, F. & Hansen, E., 1967. *A monograph on sediment transport in alluvial streams.* Copenhagen: Teknisk Forlag.

Exner, F. M., 1920. Zur Physik der Dunen. *Sitzber Akad. Wiss Wien,* IIa(129 (in German)).

Exner, F. M., 1925. Uber die Wechselwirkung zwischen Wasser und Geschiebe in Flussen. *Sitzber. Akad. Wiss Wien,* IIa(134 (in German)).

GEO-SLOPE International Ltd, 2012. *SLOPE/W 2012 slope stability analysis.* [Online]
Available at: http://downloads.geo-slope.com/geostudioresources/8/0/6/books/slope%20modeling.pdf?v=8.0.7.6129
[Accessed 20 August 2015].

Göta älvs vattenvårdförbund, 2006. *Fakta om Göta älv, En beskrivning av Göta älv och dess omgivning 2005,* Göteborg: s.n.

Göta älvs vattenvårdsförbund, 1973-2004. *Rapporter avseende Vattendragskontroll 1973-2004,* Göteborg: s.n.

Graf, W. H., 1971. Lateral Outflow Over Side Weirs. *Journal of Hydraulic Engineering, ASCE,* Vol. 113(No. 4), pp. 491-504.

Harris, K. L., 2003. *Riverbank collapse in northwestern Minnesota: an overview of vulnerable earth materials,* s.l.: Minnesota Geological Survey, University of Minnesota, St. Paul, Minnesota.

Jersby, B., 2007. *Kraftverken i Säveån.* [Online]
Available at: http://aguiden.com/alingsasguiden/meny_kraftverk.htm
[Accessed 30 July 2015].

Kasper, K. E. et al., 2005. *Accuracy of the HEC-RAS to calculate Flow Depths and Total Energy Loss with and without Bendway Weirs in a Meander Bend,* Albuquerque, New Mexico: U.S. Department of the Interior, Bureau of Reclamation.

Keller, E. A., 2011. *Introduction to Environmental Geology.* 5th ed. s.l.:Prentice Hall.

Krone, R. B., 1962. *Flume Studies of the Transport of Sediment in Esturial Shoaling Processes,* Carlifornia: Hydrologic Engineering Laboratory, University of Carlifornia Berkley.

Lane, E. W., 1955. *The importance of fluvial morphology in hydraulic engineering,* s.l.: Proc. Am. Soc. Civ. Eng. 81, Separate No. 745.

Länsstyrelserna Västra Götalands Län, n.d. *Säveåprojektet.* [Online]
Available at:

http://projektwebbar.lansstyrelsen.se/saveaprojektet/SiteCollectionDocuments/kartor.pdf
[Accessed 20 August 2015].

Laursen, E. M., 1958. Total Sediment Load of Streams. *Journal of the Hydraulics Division, American Society of Civil Engineers,* pp. 84(HY1), 1530-1 to 1530-36.

Lidmar-Bergström, K., 1998. Bergrundens ytformer. I C. Fredén (red.). *Berg och jord. Sveriges nationalatlas,* p. 44–54.

Meyer-Peter, E. & Müller, R., 1948. Formula for Bedload Transport. *International Association of Hydraulic Research 2nd Meeting, Stockholm,* p. 39.

Montgomery, D. C., Jennings, C. L. & Kulahci, M., 2015. *Time Series Analysis and Forecasting.* New Jersey: John Wiley & Sons, Inc., Hoboken.

Neil, C. R., 1967. *Stability of Coarse Bed-Material in Open Channel Flow,* s.l.: Research Council of Alberta, Edmonton, Canada.

Norconsult AB, 2015. *Översvämningskartering Utmed Säveån Utmed Säveån,* Göteborg: MSB Myndigheten för samhällsskydd och beredskap.

Osman, A. M. & Thorne, C. R., 1988. Riverbank stability analysis. I: Theory. *Journal of Hydraulic Engineering, Vol. 114, No. 2,* pp. 134-150.

Partheniades, E., 1962. *A study of Erosion and Deposition of Cohesive Soils in Salt Water,* s.l.: Berkeley PhD Dissertation.

Partheniades, E., 2010. *Cohesive Sediments in Open Channels: Properties, Transport, and Applications.* New York: Elsevier.

Pedersen, D., Cuéllar, E. & Andersson, S., 2014. *Undersökningsrapport, Skredriskkartering 2013-2014, Bathymetry Säveån,* Göteborg: Clinton AB and SGI.

Persson, G. et al., 2011. *Klimatanalys för Västra Götalands län Rapport Nr 2011-45,* Norrköping: SMHI.

Rai, R. & Singh, G., n.d. *E-Content on Slope Engineering.* [Online]
Available at: http://www.iitbhu.ac.in/faculty/min/rajesh-rai/NMEICT-

Slope/Pdf/03%20Types%20of%20slope%20failure.pdf
[Accessed 10 August 2015].

Schieber, J., n.d. *Meander Formation and Features of Meandering Streams.* [Online]
Available at:
http://www.indiana.edu/~g105lab/images/gaia_chapter_12/meander_formation.htm
[Accessed 20 August 2015].

SGI, 2012. *Landslide risks in the Göta River valley in a changing climate (Part 1,2 and 3),* Linköping: Swedish Geotechnical Institute (SGI).

Shields, A., 1936. *Application of Similarity Principles and Turbulence Research to Bedload Movement,* s.l.: transl, into English by W. P. Ott and J. C. Van Uchelen at California Institute of Technology, Pasadena California.

Taylor, D. W., 1948. *Fundamentals of Soil Mechanics.* New York: Wiley, 700 pp.

Toffaleti, F. B., 1968. A Procedure for Computation of the Total River Sand Discharge and Detailed Distribution, Bed to Surface. *Technical Report No. 5, prepared for Committee on Channel Stabilization, Corps of Engineers. U.S. Army, by U.S. Ahmy Engineer Waterways Experiment Station, Vicksburg, MS.*

Vanoni, V. A., 1975. Sedimentation Engineering. *ASCE Manuals and Reports on Engineering Practice,* Volume 54, p. 745.

White, C. M., 1940. *The Equilibrium of Grains on the Bed of an Alluvial Channel,* s.l.: Proc. Royal Soc., London, England, Series A 174, 322..

Wilcock, P. R., 2001. Toward a practical method for estimating sediment-transport rates in gravel-bed rivers. *Earth Surface Processes and Landforms 26,* p. 1395–1408.

Yang, C. T., 1973. Incipient Motion and Sediment Transport. *Journal of the Hydraulics Division, American Society of Civil Engineers,* 99(HY10), pp. 1679-1704.

Yang, C. T., 1977. The movement of sediment in rivers. *Geophysical Survey,* p. 39–68.

Yang, C. T., 1984. Unit Stream Power Equation for Gravel. *Journal of the Hydraulics Division, American Society of Civil Engineers,* 110(12), pp. 1783-1797.

Appendices

Appendix 1: Cross sections from HEC-RAS hydrodynamic simulations

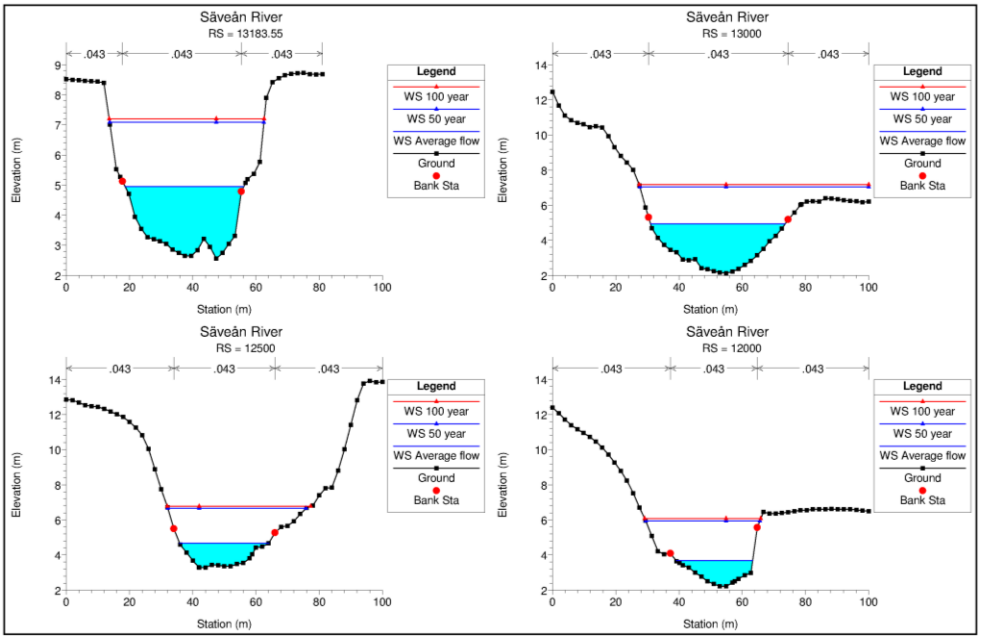

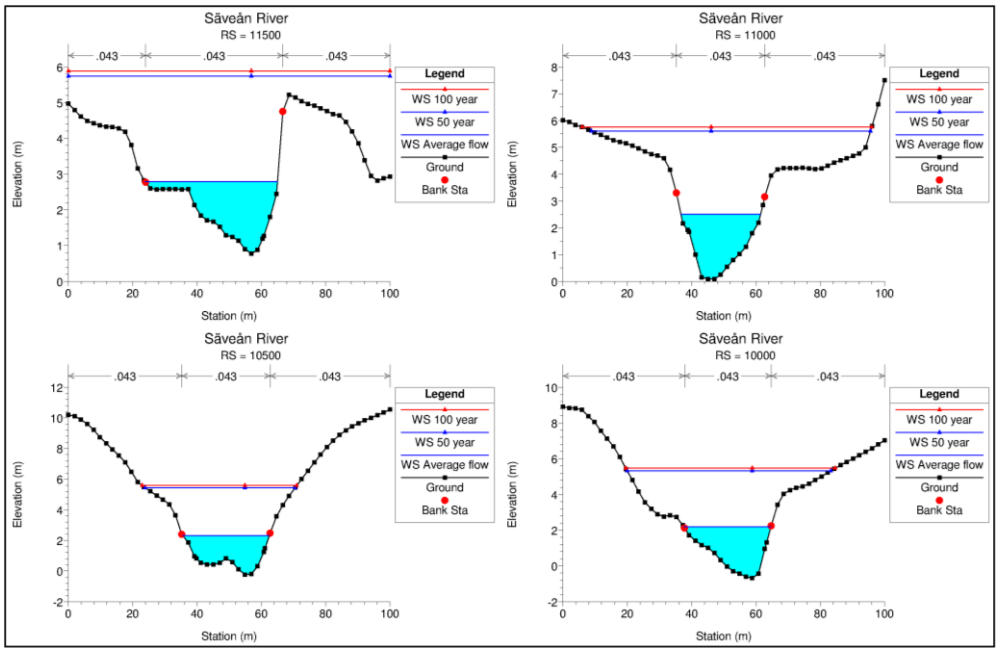
Säveån River
RS = 11500
RS = 11000
RS = 10500
RS = 10000
.043
Legend
WS 100 year
WS 50 year
WS Average flow
Ground
Bank Sta
Elevation (m)
Station (m)

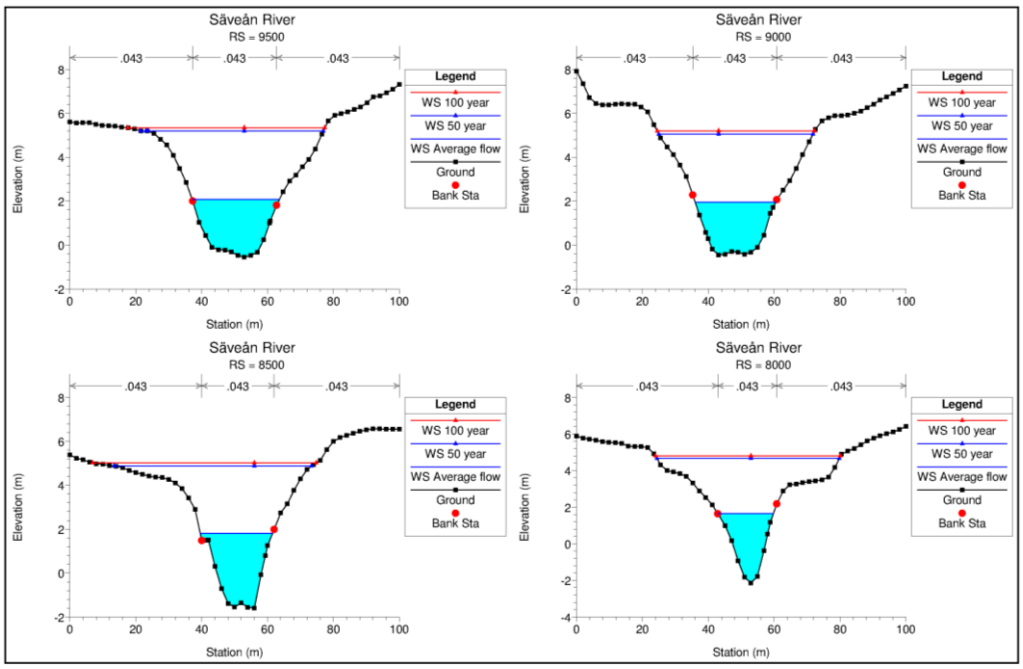
Säveån River
RS = 9500
RS = 9000
RS = 8500
RS = 8000
.043
Legend
WS 100 year
WS 50 year
WS Average flow
Ground
Bank Sta
Elevation (m)
Station (m)

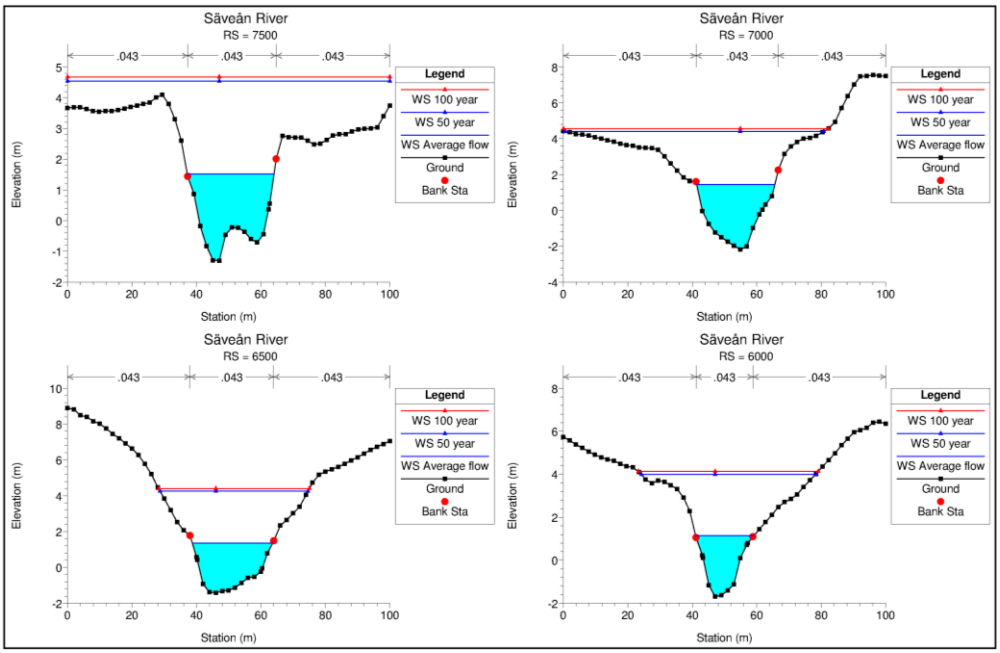
Säveån River
RS = 7500
Säveån River
RS = 7000
Säveån River
RS = 6500
Säveån River
RS = 6000
.043
.043
.043
Legend
WS 100 year
WS 50 year
WS Average flow
Ground
Bank Sta
Elevation (m)
Station (m)

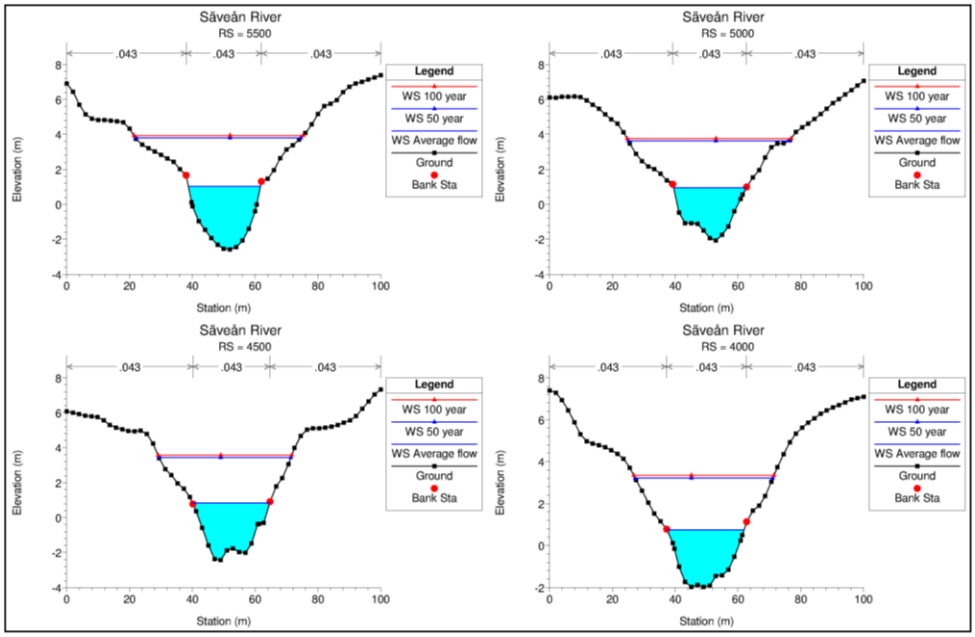
Säveån River
RS = 5500
Säveån River
RS = 5000
Säveån River
RS = 4500
Säveån River
RS = 4000
.043
.043
.043
Legend
WS 100 year
WS 50 year
WS Average flow
Ground
Bank Sta
Elevation (m)
Station (m)

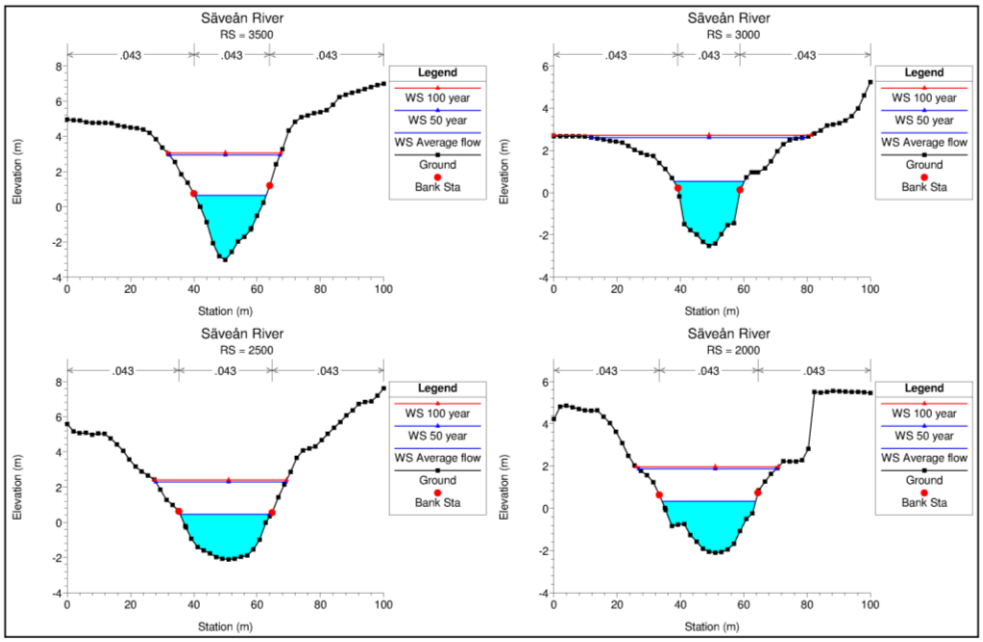
Säveån River
RS = 3500
RS = 3000
RS = 2500
RS = 2000
.043
Legend
WS 100 year
WS 50 year
WS Average flow
Ground
Bank Sta
Elevation (m)
Station (m)

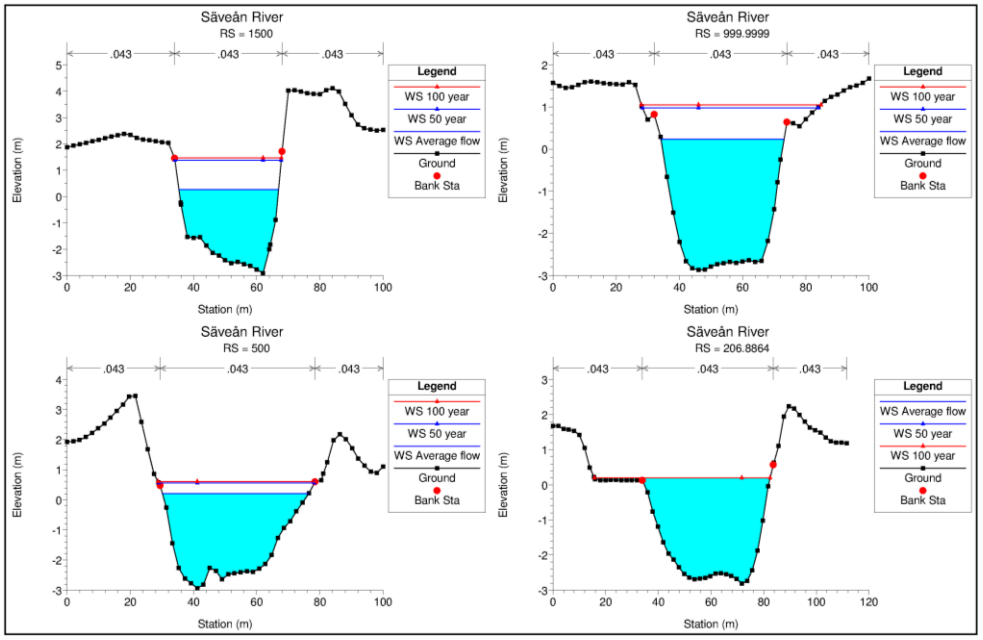
Säveån River
RS = 1500
RS = 999.9999
RS = 500
RS = 206.8864
.043
Legend
WS 100 year
WS 50 year
WS Average flow
Ground
Bank Sta
Elevation (m)
Station (m)

Appendix 2: Cross sections from SLOPE/W analysis

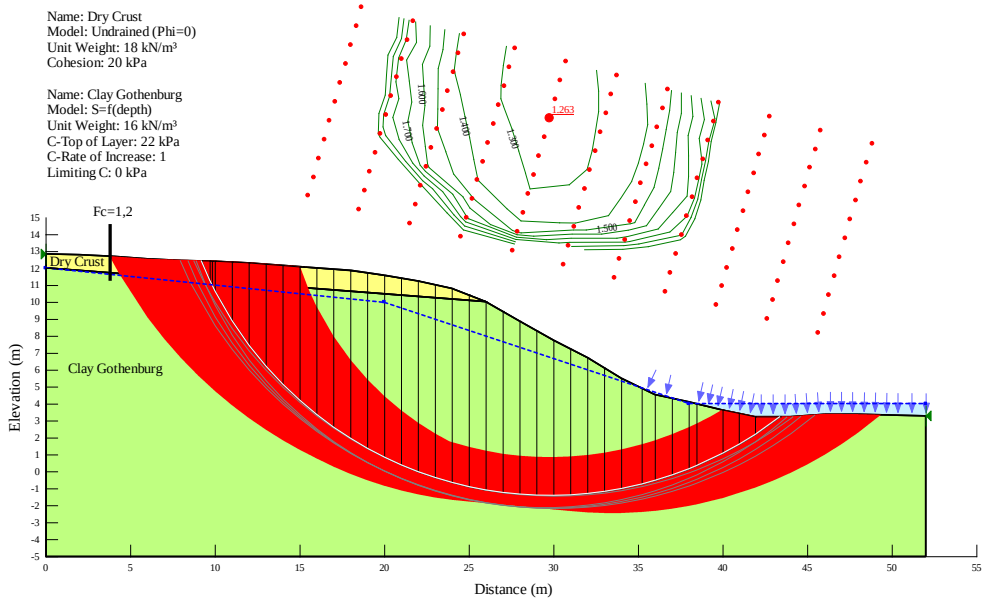

Results from SLOPE/W showing the analysis of the slope stability for the base time 2006-12-31 with given safety factor

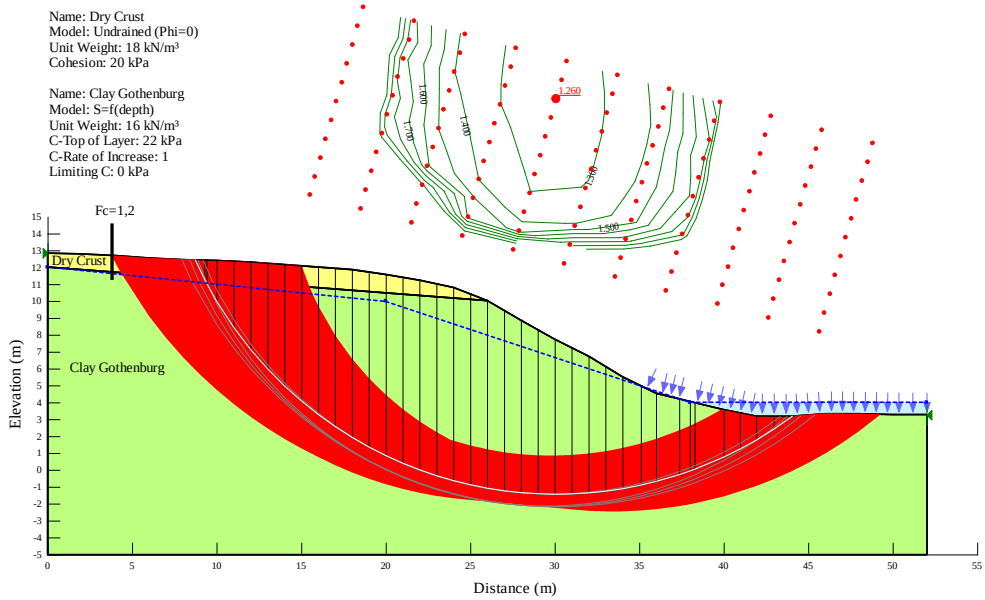

Results from SLOPE/W showing the analysis of the slope stability for the base time 2007-12-31 with given safety factor

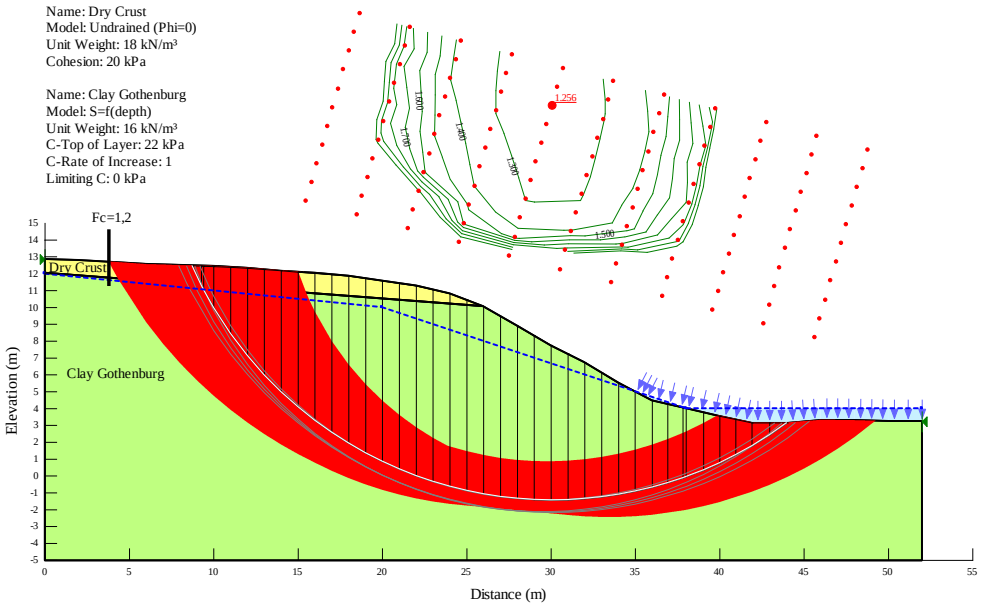

Results from SLOPE/W showing the analysis of the slope stability for the base time 2008-12-31 with given safety factor

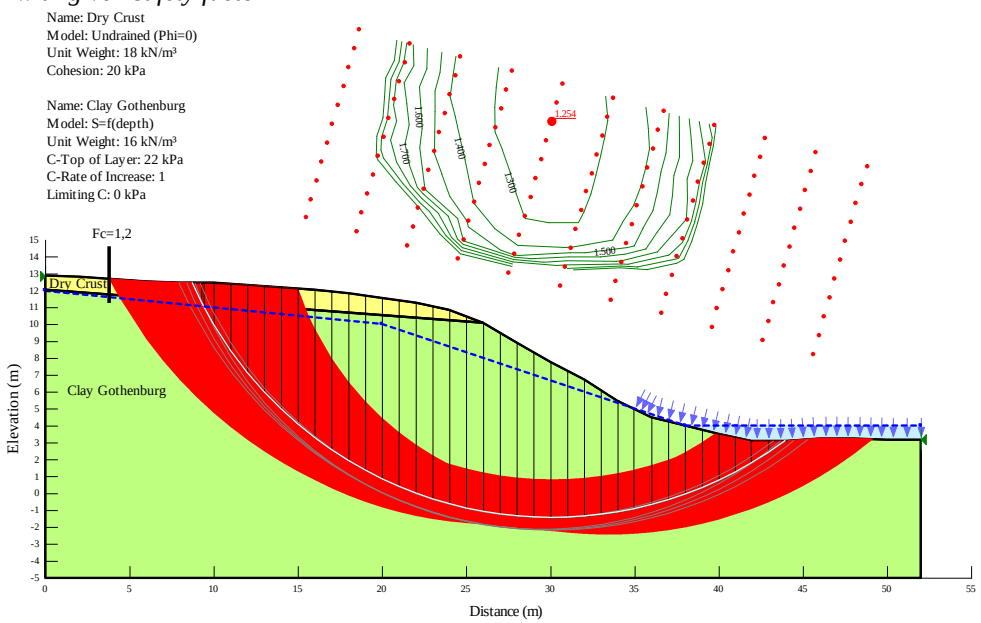

Results from SLOPE/W showing the analysis of the slope stability for the base time 2009-12-31 with given safety factor

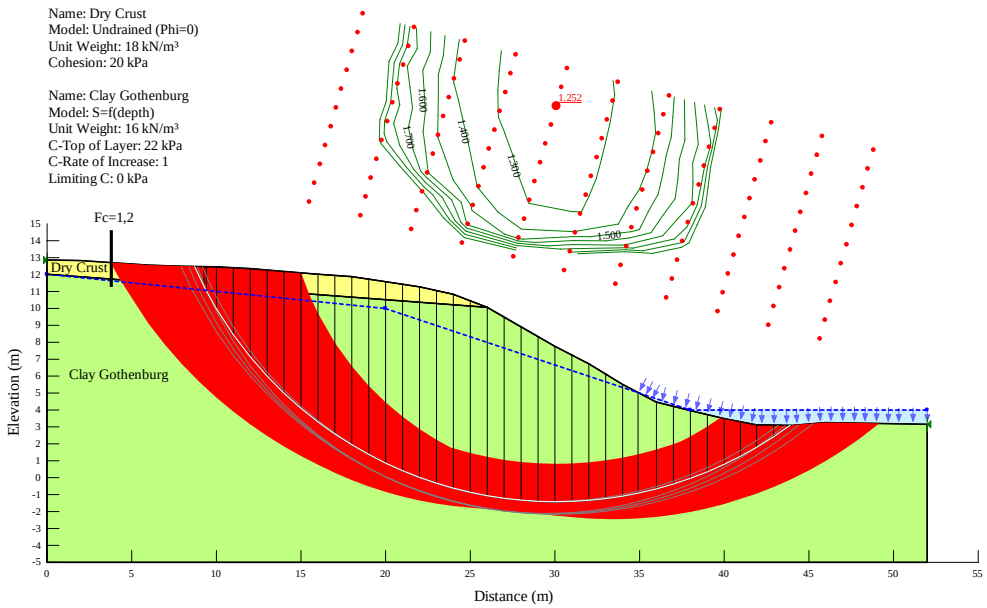

Results from SLOPE/W showing the analysis of the slope stability for the base time 2010-12-31 with given safety factor